EXPERIMENTAL STUDY OF ACTIVE CONTROL OF MDOF STRUCTURES
UNDER SEISMIC EXCITATIONS

DEPARTMENT OF CIVIL ENGINEERING
BUFFALO, NY

JULY 88

EXPERIMENTAL STUDY OF ACTIVE CONTROL
OF MDOF STRUCTURES UNDER SEISMIC EXCITATIONS

by

L.L. Chung[1], R.C. Lin[2], T.T. Soong[3] and A.M. Reinhorn[4]

July 10, 1988

Technical Report NCEER-88-0025

1 Research Associate, Dept. of Civil Engineering, State University of New York at Buffalo
2 Research Associate, Dept. of Civil Engineering, State University of New York at Buffalo
3 Professor, Dept. of Civil Engineering, State University of New York at Buffalo
4 Associate Professor, Dept. of Civil Engineering, State University of New York at Buffalo

NATIONAL CENTER FOR EARTHQUAKE ENGINEERING RESEARCH
State University of New York at Buffalo
Red Jacket Quadrangle, Buffalo, NY 14261

The National Center for Earthquake Engineering Research (NCEER) is devoted to the expansion of knowledge about earthquakes, the improvement of earthquake-resistant design, and the implementation of seismic hazard mitigation procedures to minimize loss of lives and property. Initially, the emphasis is on structures and lifelines of the types that would be found in zones of moderate seismicity, such as the eastern and central United States.

NCEER's research is being carried out in an integrated and coordinated manner following a structured program. The current research program comprises four main areas:

- Existing and New Structures
- Secondary and Protective Systems
- Lifeline Systems
- Disaster Research and Planning

This technical report pertains to Program 2, Secondary and Protective Systems, and more specifically, to a passive protective system. Protective Systems are devices or systems which, when incorporated into a structure, help to improve the structure's ability to withstand seismic or other environmental loads. These systems can be passive, such as base isolators or viscoelastic dampers; or active, such as active tendons or active mass dampers; or combined passive-active systems.

In the area of active systems, research has progressed from the conceptual phase to the implementation phase with emphasis on experimental verification. As the accompanying figure shows, the experimental verification process began with a small single-degree-of-freedom structure model, moving to larger and more complex models, and finally, to full-scale models.

Preceding page blank
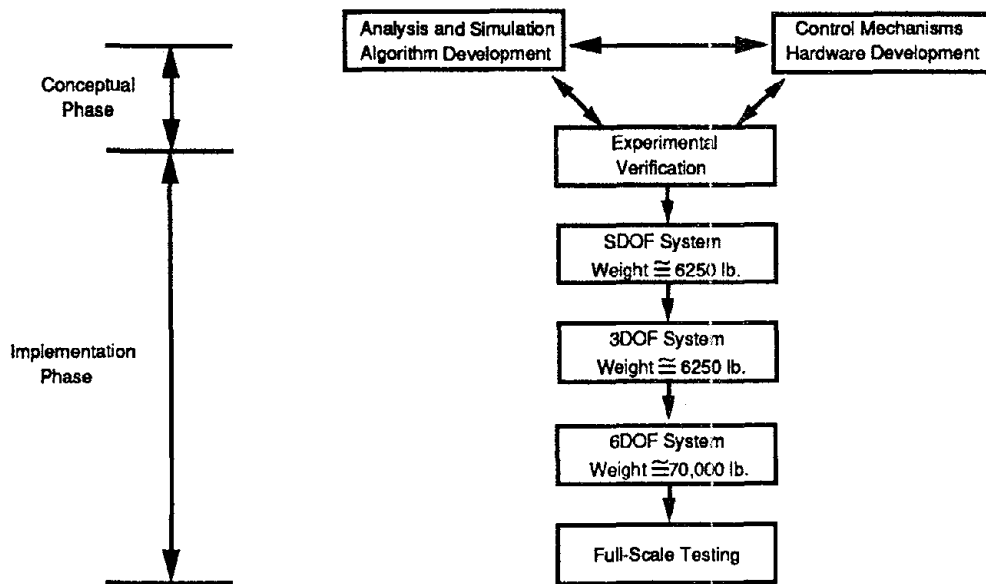
A comprehensive experimental study using the three-degree-of-freedom model has been completed and is reported in this publication. The multi-degree-of-freedom model provides opportunities for study and verification of a number of control strategies which were not possible in earlier studies. These include modal control, time delay in the modal space and control and observation spillover compensation. Moreover, further verification of a simulation procedure was carried out which gives added confidence in using simulation procedures for extrapolating active control results to more complex situations.

Active control of building structures has been extensively studied theoretically using a variety of control schemes showing varying degrees of efficiency. The demand for experimental evidence of feasibility of control of structures subjected to severe transient loads led to the present study. Structural control experiments were carried out in the laboratory using a 1:4 scaled model structure simulating a three-story frame building. The control experiments were performed using a system of prestressing tendons connected to a servo-hydraulic system and linear optimal control algorithms. The model was subjected to base motions produced by a 12'x12' shaking table, which included banded white noise and earthquake accelerograms. Results of the experiments show clearly that traditional algorithms can be implemented when proper adjustments are made. These include compensations for time delay and error accumulation in the online computation. Several new algorithms based on instantaneous optimal control were experimentally verified in this study, following new developments based on previous experiments involving single-degree-of-freedom structures. The efficiency of various algorithms is discussed along with comparisons of analytical and experimental results.

Preceding page blank

Preceding page blank

TABLE	TITLE	PAGE

Preceding page blank   xiii

INTRODUCTION

With the increase in size and flexibility of structures, various means of protection against excessive vibration have been suggested. Along with passive devices such as base isolators or viscous dampers, the method of active control has been proposed for reduction of adverse structural effects due to severe transient loads such as earthquakes [6]. Most of the previous work done in active structural control has been analytical or numerical assuming ideal conditions under which active control is implemented. While some experimental verification has been conducted with small-scale models [4,11], the demand of experimental evidence pertaining to the feasibility of structural control under realistic conditions led to the present study, which is the follow-up of a previous study for SDOF structures [2].

Initial experimental studies of structural control done by Chung et al. [2] and Lin et al [8] using linear control algorithms show that, in the presence of imperfect conditions, traditional algorithms are not feasible and in some cases produce adverse results and structural instability. As a result of these studies, several problems were identified: (a) time delay between the measured variables and the application of corrective forces can be reduced but not eliminated; (b) global optimal control is not feasible for transient loads for which the time histories are not known apriori (such as earthquakes or wind) [15-17]; (c) errors in on-line computations tend to accumulate rapidly producing control instability.

As a result of the preliminary study, Chung et al. [2] and McGreevy et al. [10] proposed and tested feasible methods of time delay compensation. Yang et al. [15,16] suggested new algorithms based on instantaneous optimum principles which enable the use of control for transient loads. Lin et al.

Preceding page blank

[7] suggested methods of updating on-line computation with measured information, thus eliminating error accumulation.

A comprehensive experimental study using a multi-degree-of-freedom structural model was performed and is reported in this paper. Using the principle of time delay compensation and updating on-line computation, the present study tested several instantaneous optimal control algorithms [15-17] along with the traditional linear global optimum feedback control [12]. Using a 1:4 scaled model of a three-story frame, the study was performed using a single control unit made of diagonal tendons prestressed by a servohydraulic actuator which was activated by a microcomputer performing real time computations.

The study was conducted using modal control with a limited number of controllers and sensors, the fact dictated by practical limitations of control implementation. However, in such a control scheme, only several modes can be controlled, usually the critical ones, while the residual modes can be adversely affected. Such problems, known as spillover [1], were included as one of the objectives of study.

The efficiency of various algorithms to reduce the response during earthquakes was studied and is presented herein. A comparison of the analytical and experimental results emphasizes some limitations of the theoretical tools to match complex damping and sampling rate differences.

CONTROL ALGORITHMS

2.1 CLASSICAL OPTIMAL CONTROL

The equation of motion of a discrete-parameter structure under earthquake excitation, $\ddot{x}_0(t)$, and active control force, $u(t)$, can be described in the state-space representation as

$$\dot{x}(t) = Ax(t) + Bu(t) + w \ddot{x}_0(t) \tag{2-1}$$

where

$$x(t) = \begin{bmatrix} x_1(t) \\ x_2(t) \end{bmatrix}, \quad A = \begin{bmatrix} 0 & I \\ -M^{-1}K & -M^{-1}C \end{bmatrix}, \quad B = \begin{bmatrix} 0 \\ M^{-1}B_1 \end{bmatrix}, \quad \text{and } w = \begin{bmatrix} 0 \\ w_1 \end{bmatrix}$$

The components $x_1(t)$ and $x_2(t)$ are the displacement and velocity vectors, respectively, M, C and K are the mass, viscous damping and stiffness matrices, respectively, and w_1 is a vector with all elements equal to -1.

In this study, the observed variables, $y(t)$, consist of storydrift displacements and storydrift velocities between adjacent floors. The output equation is therefore

$$y(t) = Ex(t) \tag{2-2}$$

where E is a 2nx2n transfer matrix.

According to the classical quadratic performance criterion, the active control force $u(t)$ is found such that the integral

$$J = 1/2 \int_0^{t_f} [x^T(t)Qx(t) + u^T(t)Ru(t)]dt \tag{2-3}$$

is minimized, where t_f is the duration of ground motion excitation, i.e., for $t > t_f$, $\ddot{x}_0 = 0$. Q is a positive semidefinite weighting matrix for the response and R is a positive definite weighting matrix for the control

rorce.

Using a linear feedback control approach and a variational procedure to minimize the performance index J [12], the active control force is linearly related to the state vector as

$$\underline{u}(t) = -G\underline{x}(t) = -R^{-1}B^{T}P\underline{x}(t) \qquad (2-4)$$

where P is obtained from the steady-state Riccati matrix equation [12]

$$PA + A^{T}P - PBR^{-1}B^{T}P + Q = 0 \qquad (2-5)$$

Expressing the control force in a feedback form,

$$\underline{u}(t) = - G_1\underline{x}_1(t) - G_2\underline{x}_2(t) \qquad (2-6)$$

and substituting in the dynamic eq. (1), the equation of motion is obtained as

$$\dot{\underline{x}}(t) = A'\underline{x}(t) + \underline{w}\,\ddot{x}_o(t) \qquad (2-7)$$

where

$$A' = \begin{bmatrix} 0 & I \\ -M^{-1}(K+B_1G_1) & M^{-1}(C+B_1G_2) \end{bmatrix}$$

Comparing matrix A in eq. (2-1) and matrix A' in eq. (2-7), the resulting controlled stiffness matrix and controlled damping matrix become, respectively,

$$K' = K + B_1G_1 \qquad (2-8a)$$

and

$$C' = C + B_1G_2 \qquad (2-8b)$$

It is seen that the effect of active control is equivalent to providing active stiffness and active damping to the uncontrolled system.

2-2

Several control algorithms were proposed and developed by Yang et al. [15-17]. They were adopted for implementation in the experimental study. The basic derivation of these control algorithms was slightly altered to include more relevant parameters and this derivation is presented here for the sake of completeness.

From structural safety point of view, the storydrift displacements are more important than the displacements relative to the base. Therefore, the storydrift vector $\underline{y}(t)$ is preferred as the control objective variables in the time-dependent cost function $J(t)$. Moreover, $\underline{y}(t)$ can be directly used as feedback variables in the control algorithms to reduce on-line computation time. Hence, the storydrift vector $\underline{y}(t)$ was used in the control algorithms as the state vector.

Based on the instantaneous optimal control law, the time-dependent performance index $J(t)$ is

$$J(t) = \underline{y}^T(t)Q\underline{y}(t) + \underline{u}^T(t)R\underline{u}(t) \tag{2-9}$$

Following the procedure described in Refs. [15-17], three control algorithms were derived. The results of these derivations are presented in Ref. [7] and summarized below.

(1) Instantaneous Optimal Open-loop Control

In this case, the control force, $\underline{u}(t)$, is regulated by the base excitation $\ddot{x}_o(t)$ alone, that is,

$$\underline{u}(t) = -[R+(\tfrac{\Delta t}{2})^2 B^T E^T Q E B]^{-1} \tfrac{\Delta t}{2} B^T E^T Q E \{t\underline{d}(t-\Delta t) + \tfrac{\Delta t}{2} \underline{w}\ddot{x}_o(t)\} \tag{2-10}$$

where T is the modal matrix whose columns are the eigenvectors of matrix A; the quantity $\underline{d}(t)$ is defined by

$$\underline{d}(t) = \exp(\theta \Delta t)[\underline{d}(t-\Delta t) + T^{-1}(B\underline{u}(t) + \underline{w}\ddot{x}_o(t))\Delta t] \qquad (2\text{-}11a)$$

or

$$\underline{d}(t) = \exp(\theta \Delta t)T^{-1}(E^{-1}\underline{y}(t) + \frac{\Delta t}{2}(B\underline{u}(t) + \underline{w}\ddot{x}_o(t))] \qquad (2\text{-}11b)$$

in which $\theta = T^{-1}AT$. When the vector $\underline{d}(t)$ is determined using eq. (2-11a), only the measurement of the base acceleration is needed to determine the control force. However, this control algorithm could not be implemented experimentally [7,8]. This can be largely attributed to errors which were introduced into computation of the vector $\underline{d}(t)$ as given by eq. (2-11a) due to time delay and measurement errors in the actual control process, and these errors were accumulated in the entire control process. Hence, in order to reduce the effect of these errors on control computation, the vector $\underline{d}(t)$ was corrected by using measured state variables. Thus, instead of using eq. (2-11a), $\underline{d}(t)$ was determined by eq. (11b) which makes use of measured state variables, $\underline{y}(t)$.

(2) Instantaneous Optimal Closed-loop Control

The control force, $\underline{u}(t)$, in this case is regulated by the state vector, $\underline{y}(t)$, alone, that is,

$$\underline{u}(t) = -\frac{\Delta t}{2} R^{-1}B^TE^TQ\underline{y}(t) \qquad (2\text{-}12)$$

(3) Instantaneous Optimal Open-closed-loop Control

Let the control force $\underline{u}(t)$ be regulated by both the state vector, $\underline{y}(t)$, and base acceleration $\ddot{x}_o(t)$. One obtains

$$\underline{u}(t) = \frac{\Delta t}{4} R^{-1}B^TE^T\Lambda E\{E^{-1}\underline{y}(t) + T\underline{d}(t-\Delta t) + \frac{\Delta t}{2}\underline{w}\ddot{x}_o(t))\} \qquad (2\text{-}13)$$

where

$$\Lambda = -[I + \frac{\Delta t^2}{8} QEBR^{-1}B^TE^T]^{-1}Q \qquad (2\text{-}14)$$

2-4

Using these instantaneous optimal control algorithms, the state vector can be constructed by the same relation

$$\underline{y}(t) = L\{T\underline{q}(t-\Delta t) + \frac{\Delta t}{2} \underline{w} \ddot{\underline{x}}_o(t)\}$$

(2-15)

where L is a 2nx2n matrix which characterizes control efficiency. For the same control parameters, the matrix L is the same in all three control algorithms. Thus, the three control algorithms are theoretically identical when all the control parameters are the same.

MODAL CONTROL

A civil engineering structure is in nature a continuum whose dynamic behavior is generally described by a distributed-parameter system. In order to apply optimal control using a state-space formulation, the structure is usually discretized by means of a lumped-parameter approximation or modal expansion techniques. However, the full-order discretized system is still too complicated with a large or infinite number of degrees of freedom. Hence, further model reduction is in general necessary.

As in the case of classical linear optimal feedback control, the order of computation in solving the Riccati matrix equation (eq. 2-5) is the square of the order of the system equation. Thus, the use of reduced-order models would reduce significantly required off-line and on-line computation time.

Due to inherent performance limitations, a servo-controller cannot react fast enough to control certain higher order modes. Therefore, it is usually not practical to design control laws over the entire frequency spectrum. Modal control is introduced to control some critical modes while leaving the residual modes uncontrolled. It is not necessary for the controlled modes to be the first few modes of the structure. Because of implementation feasibility and economic considerations, the number of controllers and sensors is severely limited in comparison with the dimension of the structure. Consequently, the induced control and observation spillover may degrade the structural performance seriously [1,13]. Thus actions should be taken to reduce the influence of control and observation spillover.

Preceding page blank

With modal matrix as the transformation matrix, the equation of motion, eq. (1), can be rewritten in the modal coordinates $\eta(t)$ as

$$\bar{M}\ddot{\eta}(t) + \bar{C}\dot{\eta}(t) + \bar{K}\eta(t) = \Phi^T B_1 u(t) + \Phi^T W_1 \ddot{x}_0(t) \tag{3-1}$$

where the superscript '$^-$' denotes the corresponding modal quantities. If the modal coordinates $\eta(t)$ are partitioned into the controlled critical modes $\eta_c(t)$ and the uncontrolled residual modes $\eta_r(t)$, the physical and modal coordinates are related by

$$x_1(t) = \begin{bmatrix} x_{1c}(t) \\ x_{1r}(t) \end{bmatrix} = \Phi\eta(t) = [\Phi_c \ \Phi_r] \begin{bmatrix} \eta_c(t) \\ \eta_r(t) \end{bmatrix} = \begin{bmatrix} \Phi_{cc} & \Phi_{cr} \\ \Phi_{rc} & \Phi_{rr} \end{bmatrix} \begin{bmatrix} \eta_c(t) \\ \eta_r(t) \end{bmatrix} \tag{3-2}$$

and the equation of motion can also be partitioned into

$$M_c\ddot{\eta}_c(t) + C_c\dot{\eta}_c(t) + K_c\eta_c(t) = \Phi_c^T B_1 u(t) + \Phi_c^T W_1 \ddot{x}_0(t) \tag{3-3}$$

and

$$M_r\ddot{\eta}_r(t) + C_r\dot{\eta}_r(t) + K_r\eta_r(t) = \Phi_r^T B_1 u(t) + \Phi_r^T W_1 \ddot{x}_0(t) \tag{3-4}$$

Using the linear optimal control approach, $u(t)$ can be determined through variational procedures as

$$u(t) = - G_1 \eta_c(t) - G_2 \dot{\eta}_c(t) \tag{3-5}$$

If all state variables are available from measurements, the coordinates of the critical modes can be constructed from the physical coordinates from eq. (3-2) as

$$\eta_c(t) = (\Phi_{cc} - \Phi_{cr}\Phi_{rr}^{-1}\Phi_{rc})^{-1} [x_{1c}(t) - \Phi_{cr}\Phi_{rr}^{-1}x_{1r}(t)] \tag{3-6}$$

By examining the dynamic equations (3-3) and (3-4), the effect of feedback control force $u(t)$ on the critical modes is to supply active damping and

active stiffness. However, to the residual modes, its effect is to provide an extra and possibly an adverse excitation in addition to the dynamic loading.

Considering the action of the feedback force, the effective modal stiffness and damping matrices are, respectively,

$$K' = \begin{bmatrix} K_c + \Phi_c^T B_1 G_1 & 0 \\ \\ \Phi_r^T B_1 G_1 & K_r \end{bmatrix}$$ (3-7)

and

$$C' = \begin{bmatrix} C_c + \Phi_c^T B_1 G_2 & 0 \\ \\ \Phi_r^T B_1 G_2 & C_r \end{bmatrix}$$ (3-8)

It is found that eigenproperties of the residual modes, related to K_r and C_r only, are invariant for the controlled system. Provided that critical modes can be perfectly constructed from measurements, stability of the residual modes is not influenced by the feedback force. This was illustrated also experimentally as shown in the next section. Furthermore, control spillover $\Phi B_1 u(t)$ can be eliminated if the controllers are implemented in such a way that the control forces are applied at the nodal points of all residual mode shapes. However, this is not usually feasible [13].

3.2 OBSERVATION SPILLOVER

If only a part of the state variables, $x_{1c}(t)$, is available for measurement, the critical modal coordinates can be reconstructed by assuming that $x_{1c}(t)$ is contributed by the critical modes only, i.e.,

$$\eta_c(t) = \Phi_{cc}^{-1} x_{1c}(t)$$ (3-9)

3-3

$$\underline{u}(t) = -G_1\underline{\eta}_c(t) - G_2\dot{\underline{\eta}}_c(t)$$

$$= - G_1\underline{\eta}_c(t) - G_2\dot{\underline{\eta}}_c(t) - G_1\Phi_{cc}^{-1}\Phi_{cr}\underline{\eta}_r(t) - G_2\Phi_{cc}^{-1}\Phi_{cr}\dot{\underline{\eta}}_r(t) \qquad (3-10)$$

The effective modal stiffness and damping matrices for the controlled system are, respectively,

$$K' = \begin{bmatrix} K_c + \Phi_c^T B_1 G_1 & \Phi_c^T B_1 G_1 \Phi_{cc}^{-1}\Phi_{cr} \\ \\ \Phi_r^T B_1 G_1 & K_r + \Phi_r^T B_1 G_1 \Phi_{cc}^{-1}\Phi_{cr} \end{bmatrix} \qquad (3-11)$$

and

$$C' = \begin{bmatrix} C_c + \Phi_c^T B_1 G_2 & \Phi_c^T B_1 G_2 \Phi_{cc}^{-1}\Phi_{cr} \\ \\ \Phi_r^T B_1 G_2 & C_r + \Phi_r^T B_1 G_2 \Phi_{cc}^{-1}\Phi_{cr} \end{bmatrix} \qquad (3-12)$$

The eigenproperties of the residual modes are no longer the same as expected as seen from the coupled terms K'_{22} and C'_{22} in eqs. (3-11) and (3-12) which are influenced by the feedback control force and by the eigenproperties of the critical modes. Therefore, the observation spillover may cause instability in the residual modes. As in the case of control spillover, observation spillover can also be eliminated if the sensors are mounted at the nodal points of the residual mode shapes, but again, this is not usually feasible [13].

TIME DELAY COMPENSATION

If the displacement feedback force lags the displacement by τ_x in time while velocity feedback force lags the velocity by $\tau_{\dot{x}}$ in time, their corresponding phase lags for the i-th mode are $\omega_i \tau_x$ and $\omega_i \tau_{\dot{x}}$, respectively. Fig. 4-1 shows the relationship between feedback forces and responses in the phase space. With the phase shift, the displacement feedback force may be resolved to produce positive active stiffness and negative active damping while the velocity feedback force may be resolved to produce positive active stiffness and positive active damping. Due to the existence of negative active damping, control effects are diminished for the real system as compared to the ideal one. Even worse, time delay will cause instability if the resultant damping force is negative. Since phase lag is proportional to the delay time and modal frequency, the effect of time delay may be serious for higher modes even with small amounts of time delay.

Time delay can be compensated in the modal domain by a phase shift method which was developed for single-degree-of-freedom systems [2] and previously compared experimentally with several other methods [10]. The control force contributed by the i-th mode can be expressed as

$$u_i(t) = -g_{1i}\eta_i(t) - g_{2i}\dot{\eta}_i(t) = -g'_{1i}\eta_i(t-\tau_x) - g'_{2i}\dot{\eta}_i(t-\tau_{\dot{x}}) \qquad (4\text{-}1)$$

where g_{1i} and g_{2i} are the modified displacement and velocity feedback gain factors, respectively, with time delay compensation. The modified feedback gain factors are determined so that the same control effect can be achieved.

Due to phase shift, the displacement feedback force contributed by the i-th mode can be resolved into the displacement and velocity components as

4-1
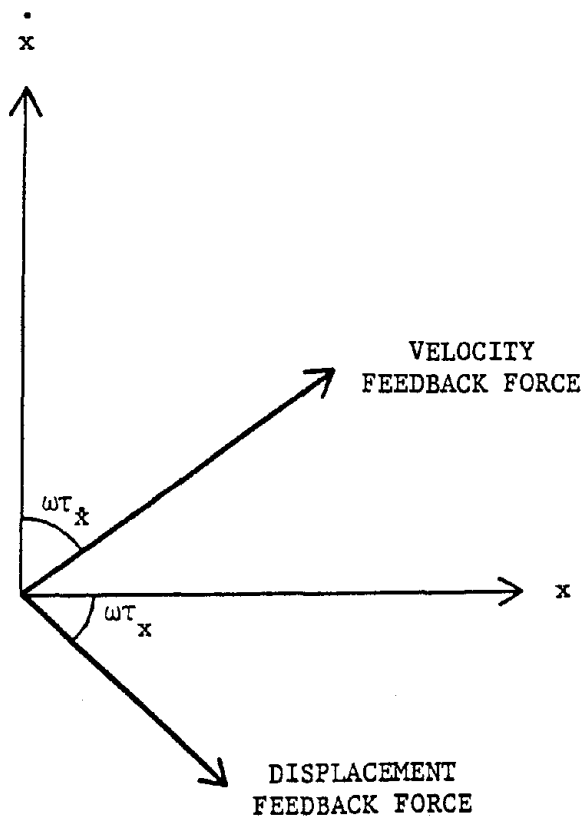
FIGURE 4-1 Phasor Diagram of Feedback Forces and Responses

$(g'_{1i}\cos\omega_i\tau_x)\eta_i$ and $(-g'_{1i}\sin\omega_i\tau_x)\eta_i/\omega_i$, respectively. Similarly, the displacement and velocity components of the velocity feedback force contributed by the i-th mode are, respectively, $(g'_{2i}\sin\omega_i\tau_x)\omega_i\eta_i$ and $(g'_{2i}\cos\omega_i\tau_x)\dot{\eta}_i$. In order to make the real system equivalent to the ideal one, the relationship between feedback gains for the real system and those for the ideal system can be established such that both systems have the same active stiffness and active damping. Thus, the modified feedback gains are obtained:

$$[g'_{1i} \quad g'_{2i}] = [g_{1i} \quad g_{2i}] \begin{bmatrix} \cos\omega_i\tau_x & -(1/\omega_i)\sin\omega_i\tau_x \\ \\ \omega_i\sin\omega_i\tau_x & \cos\omega_i\tau_x \end{bmatrix}^{-1} \qquad (4\text{--}2)$$

From a pre-calculated feedback gain matrix for the ideal system, the modified real system feedback gain matrix can be constructed using the transformation given by eq. (4-2).

4-3
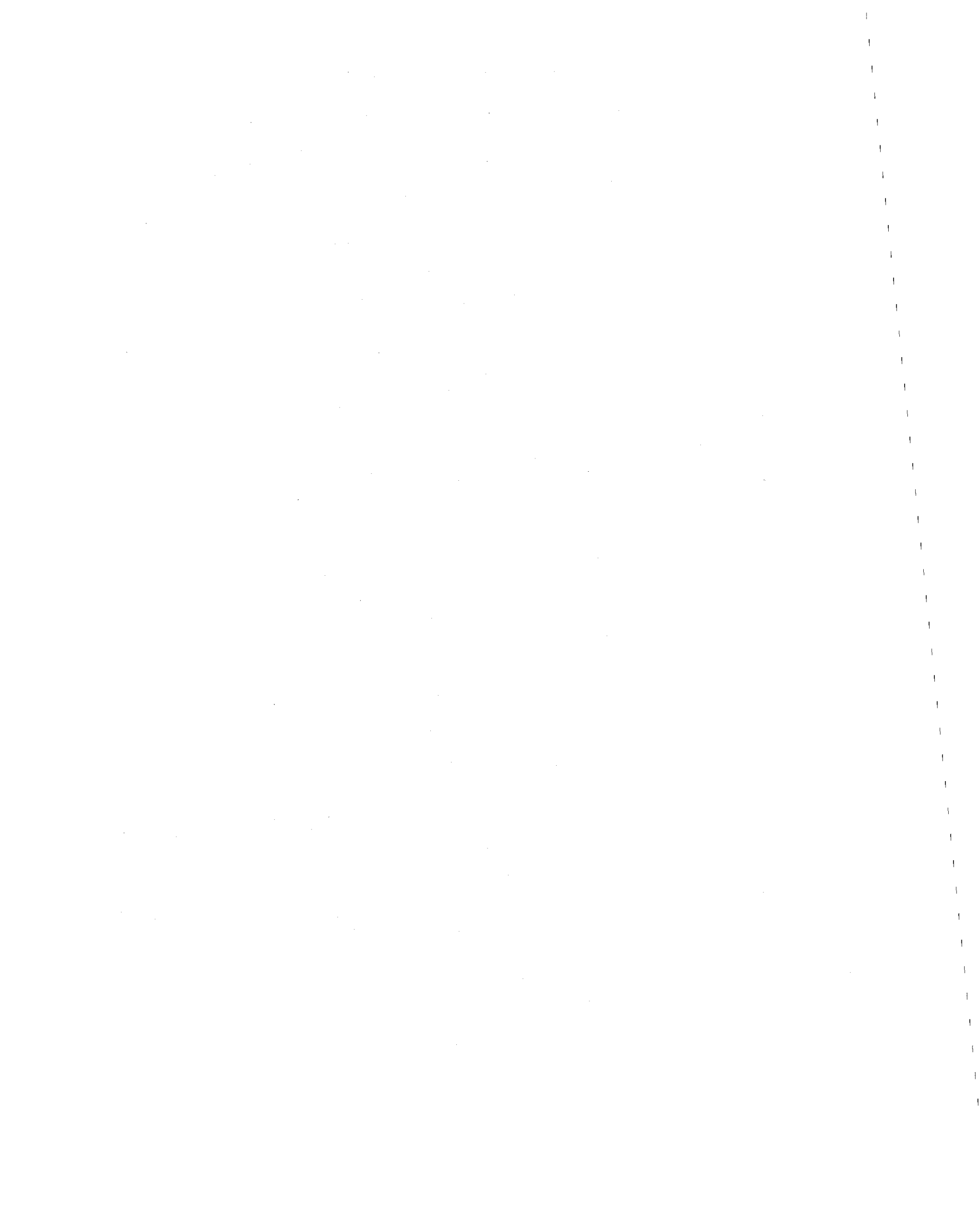
EXPERIMENTAL STUDY

5.1 EXPERIMENTAL SET-UP AND MODEL STRUCTURE

The basic experimental set-up used in this study consisted of a three-story 1:4 scale frame with one tendon control device implemented to the first floor (Fig. 5-1). The control was supplied by a servocontrolled hydraulic actuator through a system of tendons. A detailed description of the set-up and the identification studies are found in Refs. [3,7,14].

The state variable measurements were made by means of strain gage bridges installed on the columns just below each floor slab. For each set of the strain gage bridges, the signal from one strain gage bridge was used as the signal of measured storydrift displacement between adjoining stories, while the signal from the second set was further passed through an analog differentiator to yield measured storydrift velocity. The base acceleration and the absolute acceleration of each floor were directly measured by the use of accelerometers installed at the base of the structure and on the floor slabs. The transducers and instrumentation system is shown in Fig. 5-2. A block diagram showing the measurement system and the control procedure is given in Fig. 5-3.

5.2 BASE MOTION

The model was shaken by the earthquake simulator with banded white noise and an earthquake accelerogram. Under white noise excitation, modal properties were identified from the frequency response functions for system identification. Moreover, it provided a preliminary examination of the system performance including structural, sensor and controller dynamics for more realistic inputs that were to follow. The N-S component of El-Centro acceleration record was used in the experiment, however, it was scaled to

Preceding page blank
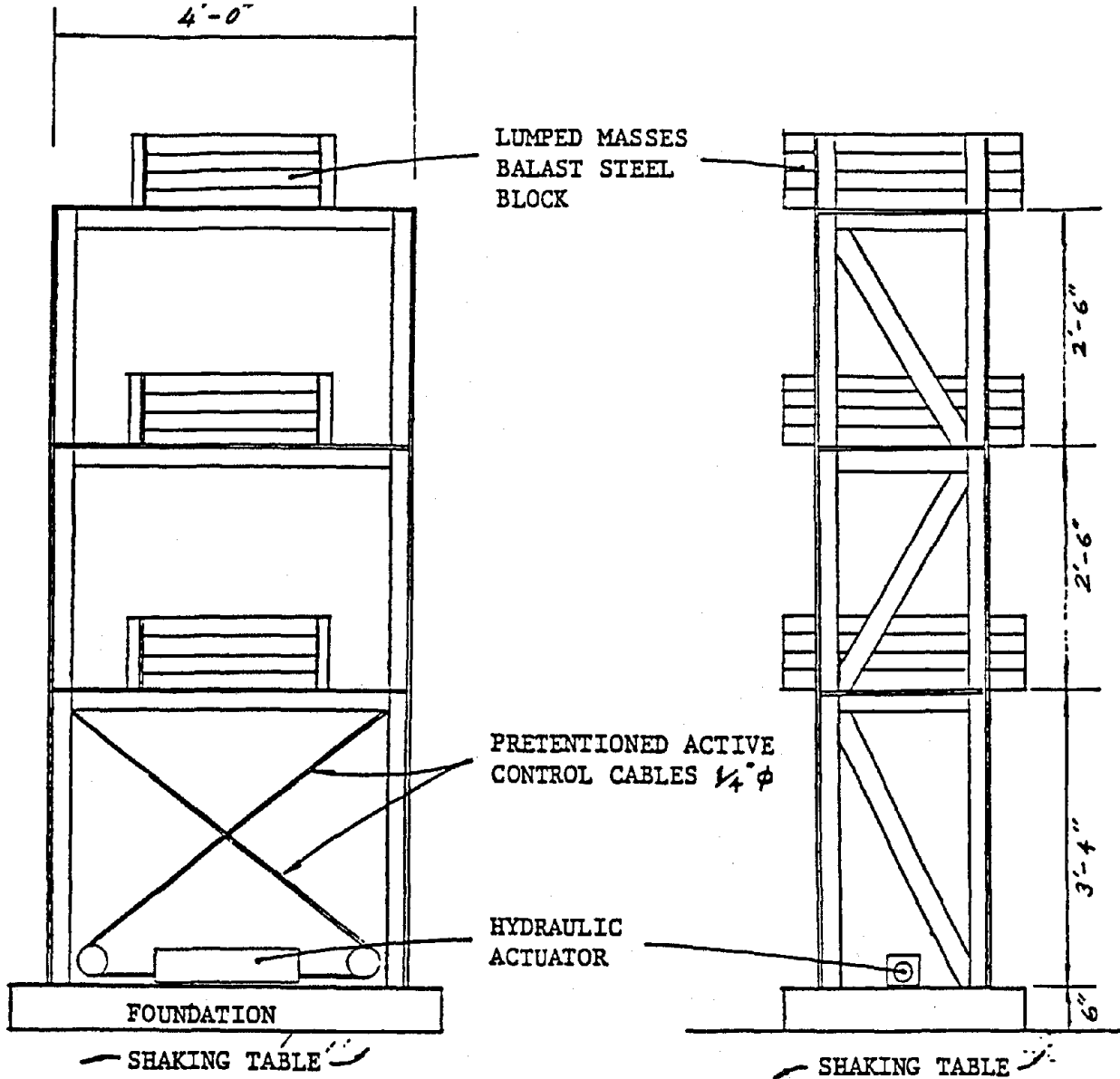
FIGURE 5-1   Configuration of the Model Structure for MDOF System
(Total Weight 6250 lbs.)

N

● ACCELEROMETER

H STRAIN GAGE

LVDT

□ LOAD CELL

STEEL BLOCK

ACTUATOR

CHANNEL BEAM

CONCRETE BLOCK
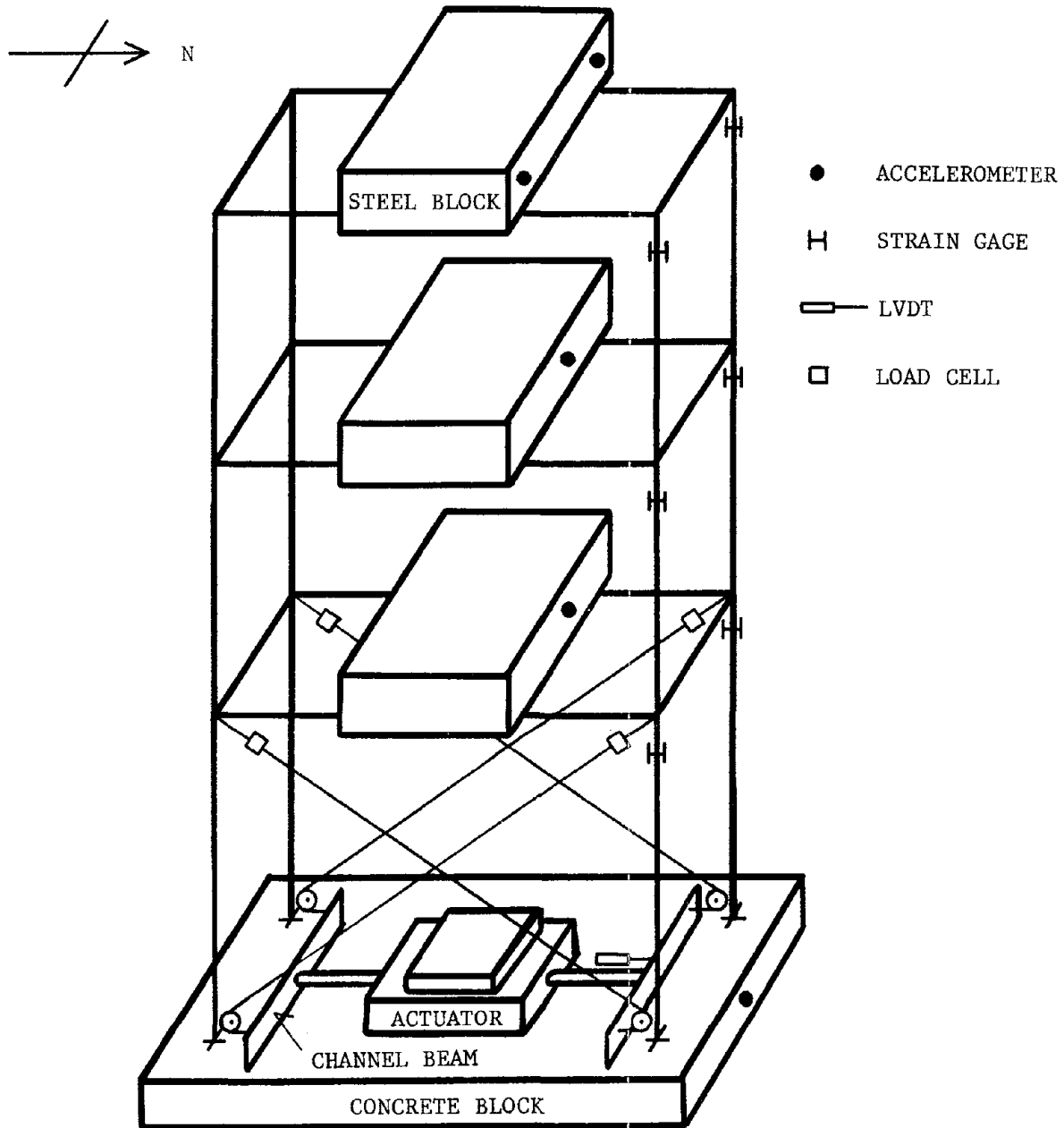
FIGURE 5-2 Transducers Instrumentation System
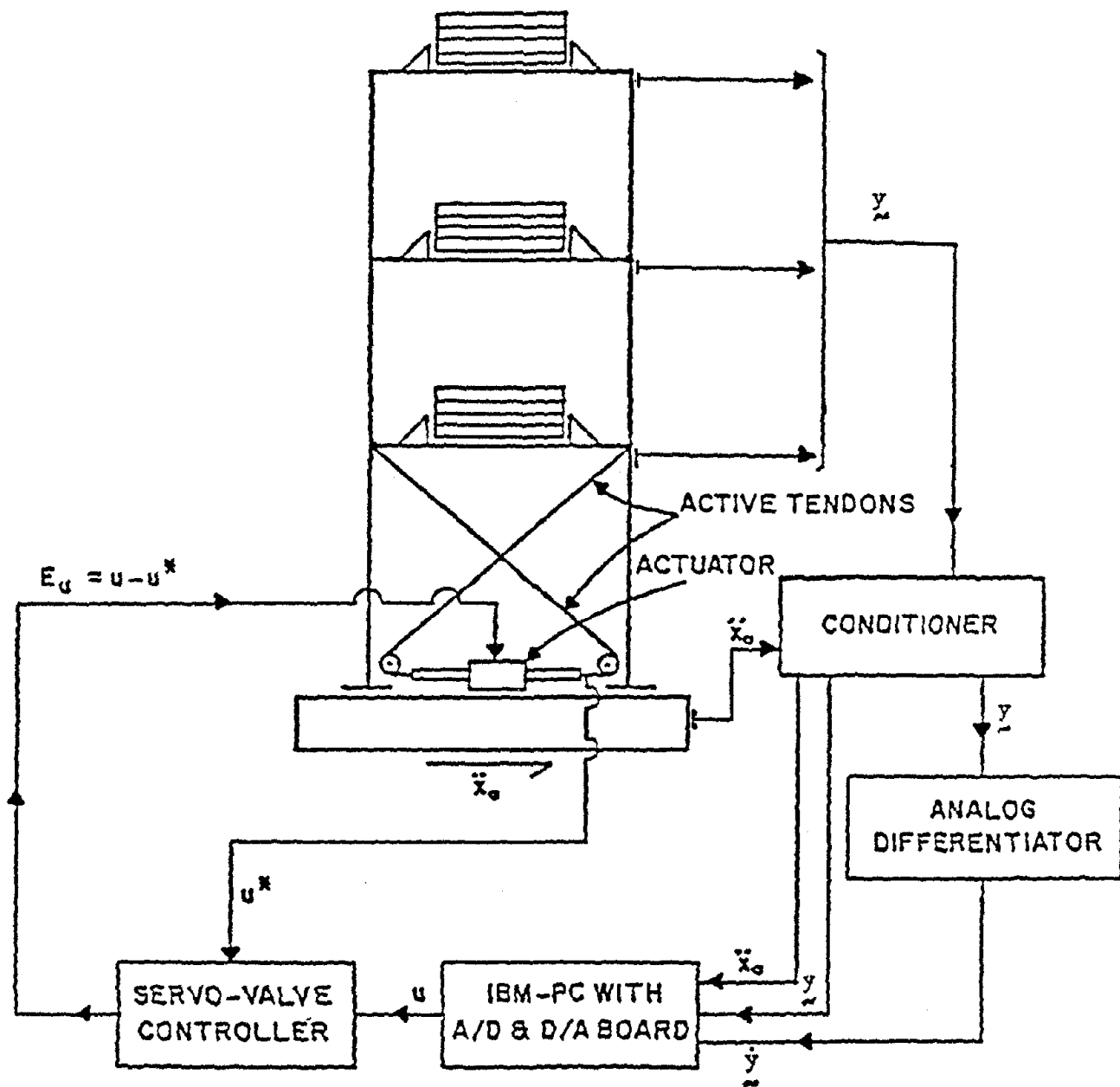
FIGURE 5-3 Block Diagram of Control System

25% of its actual intensity to prevent inelastic deformations in the model structure during uncontrolled vibrations. The reproduced time history and the frequency distribution of the scaled down El Centro excitation are shown in Fig. 5-4.

5.3 EXPERIMENTAL RESULTS

The classical closed-loop optimal control was first studied with all three modes under control. After carrying out the variational procedure, it was found that there was only a slight increase in natural frequencies (stiffness) but damping factors were increased from 1.62%, 0.39% and 0.36% to 12.77%, 12.27% and 5.45% (Tables 5-1 and 5-2).

The spillover was investigated by selecting the first fundamental mode as the controlled critical mode. The critical modal quantities were reconstructed from the measurements at all floors. The effect of spillover to the residual modes was studied. When fewer output measurements were available, the estimated critical modal quantities were actually affected by the observation spillover to the residual modes. Even worse, time delay was compensated as if the outputs were contributed by the critical modes alone. The combined effect of observation spillover and time delay made the system unstable.

When the first fundamental mode was the only controlled critical mode, the modal quantities were recovered from measurements at all three floors. In the presence of modelling errors (mode shapes were not exactly orthogonal) and measurement noise, the first modal quantities could not be reconstructed perfectly and small contribution of the residual modes to the feedback signal was unavoidable. Because of small stability margins (small damping factors) for the second and third modes, the model structure was very sensitive to these errors. To circumvent this problem, the command control signal was passed through a low-pass filter before driving the

TABLE 5-1   Parameters of the Model Structure

mass matrix M (lb-sec^2/in.)	$\begin{bmatrix} 5.6 & 0 & 0 \\ 0 & 5.6 & 0 \\ 0 & 0 & 5.6 \end{bmatrix}$
stiffness matrix K (lb/in.)	$\begin{bmatrix} 15649 & -9370 & 2107 \\ -9370 & 17250 & -9274 \\ 2107 & -9274 & 7612 \end{bmatrix}$
damping matrix C (lb-sec/in.)	$\begin{bmatrix} 2.185 & -0.327 & 0.352 \\ -0.327 & 2.608 & -0.015 \\ 0.352 & -0.015 & 2.497 \end{bmatrix}$
modal frequency $\underset{\sim}{\omega}$ (Hz)	$\begin{bmatrix} 2.24 \\ 6.83 \\ 11.53 \end{bmatrix}$
modal damping factor $\underset{\sim}{\zeta}$ (%)	$\begin{bmatrix} 1.62 \\ 0.39 \\ 0.36 \end{bmatrix}$
tendon stiffness k_c (lb/in.)	2124
tendon inclination α ($^\circ$)	36
modal matrix Φ	$\begin{bmatrix} 0.262 & 0.743 & 0.583 \\ 0.568 & 0.373 & -0.728 \\ 0.780 & -0.555 & 0.360 \end{bmatrix}$

TABLE 5-11   Parameters of Control System

PARAMETERS	THREE CONTROLLED MODES	ONE CONTROLLED MODE
response weighting matrix Q [1]	$\begin{bmatrix} K & 0 \\ 0 & 0 \end{bmatrix}$	
control weighting matrix R [2]	$20\,k_c$	
modal frequency $\underset{\sim}{\omega}$ (Hz)	$\begin{bmatrix} 2.28 \\ 6.94 \\ 11.56 \end{bmatrix}$	$\begin{bmatrix} 2.28 \\ 6.83 \\ 11.53 \end{bmatrix}$
modal damping factor $\underset{\sim}{\zeta}$ (%)	$\begin{bmatrix} 12.77 \\ 12.27 \\ 5.45 \end{bmatrix}$	$\begin{bmatrix} 12.77 \\ 0.39 \\ 0.36 \end{bmatrix}$
time delay τ_x, $\tau_{\dot{x}}$ (msec)	35	88
feedback gain matrix G^T	$\begin{bmatrix} 0.1857 \\ -0.1571 \\ 0.0641 \\ 0.0171 \\ 0.0021 \\ 0.0055 \end{bmatrix}$	$\begin{bmatrix} 0.0056 \\ 0.0123 \\ 0.0157 \\ 0.0027 \\ 0.0059 \\ 0.0076 \end{bmatrix}$

[1] K is structural stiffness matrix
[2] K_c is tendon stiffness
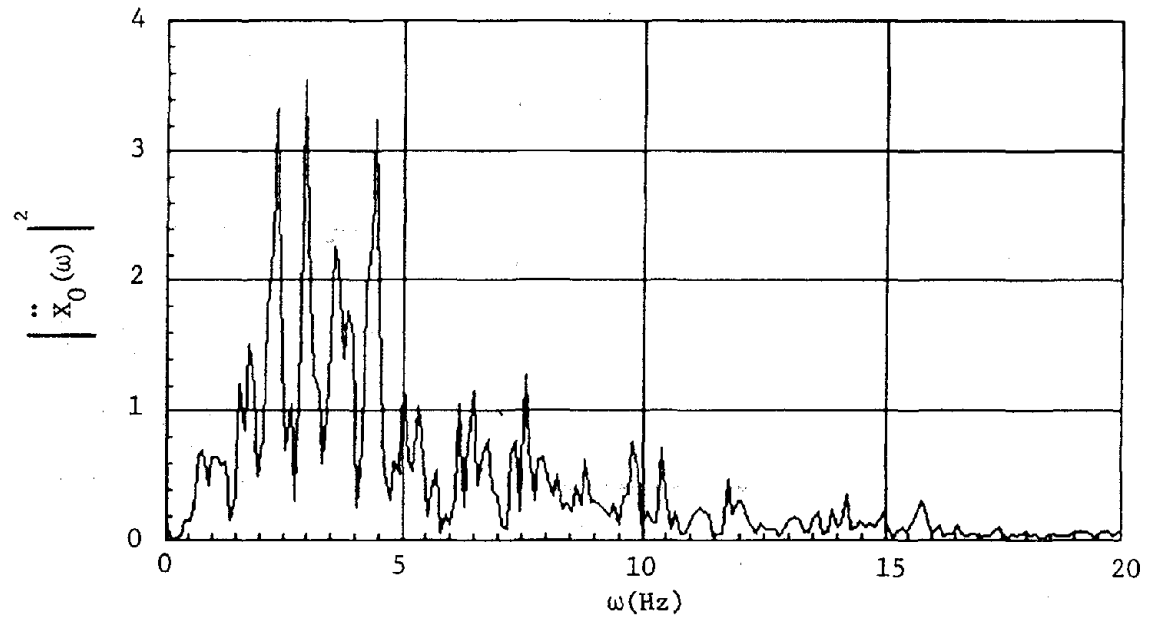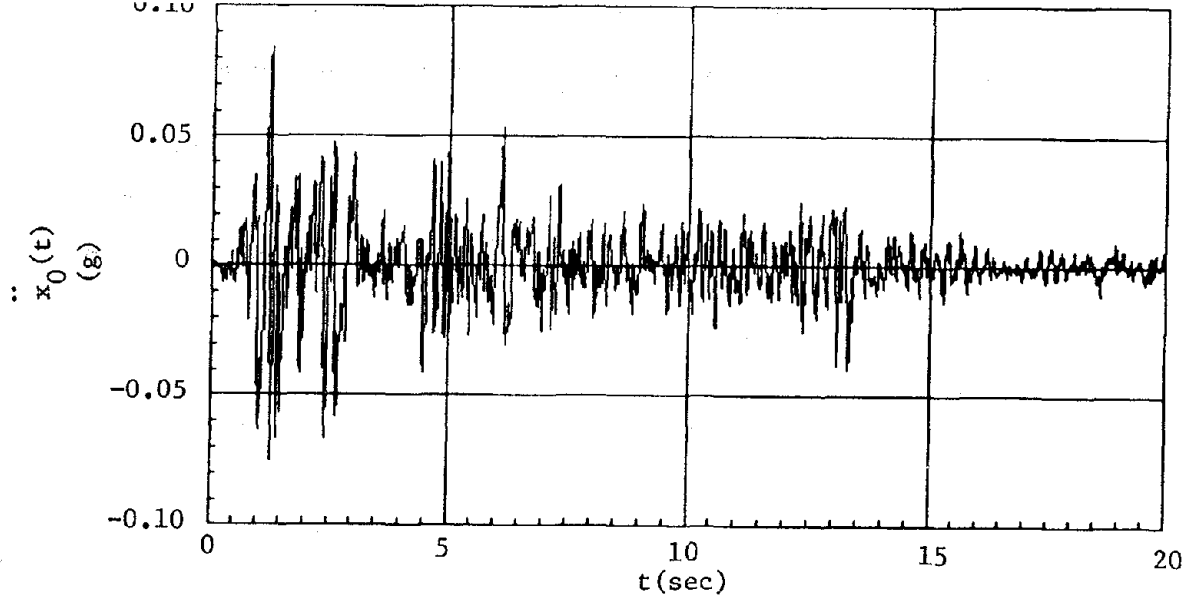
FIGURE 5-4 Scaled-down El Centro Excitation Used for Experimental Study

actuator in order to eliminate the effect of the residual modes. However, no perfect filter exists; the higher the order is the filter, the sharper is the cutoff frequency, but the longer is the time delay. As a compromise, a third-order Butterworth filter with a cutoff frequency of 5 Hz was selected, but time delay was increased from 35 msec. to 88 msec.

Acceleration frequency response functions as shown in Figs. 5-5 through 5-7 were constructed by using banded white noise excitation. For the three controlled modes, significant damping effect (large active damping) was reflected from a decrease in peak magnitude, but peak frequencies made a shift to the right due to its small active stiffness. It was shown that all three modes were under control with one controller in the presence of time delay. For the case of one controlled mode, the peak of the first mode was decreased but the peaks of the second and third modes were increased. Due to the effect of the control spillover, the performance of the controlled system was not better than that of the uncontrolled one.

Under El Centro excitation, significant reduction in acceleration was achieved with three controlled modes. In addition to the reduction in peak magnitudes, the effect of active damping was clearly evident due to control execution but the excitation frequency was distributed over all three modes. Due to control spillover, the control effect was greatly degraded (Figs. 5-8 through 5-10).

The instantaneous optimal control algorithms were studied with all three modes under control using the seismic excitation. Since a single control force applied to the first floor was only considered for all control algorithms, the weighting matrix R in eq. (2-9) is a scalar constant and the weighting matrix Q is a 6x6 diagonal matrix, that is,
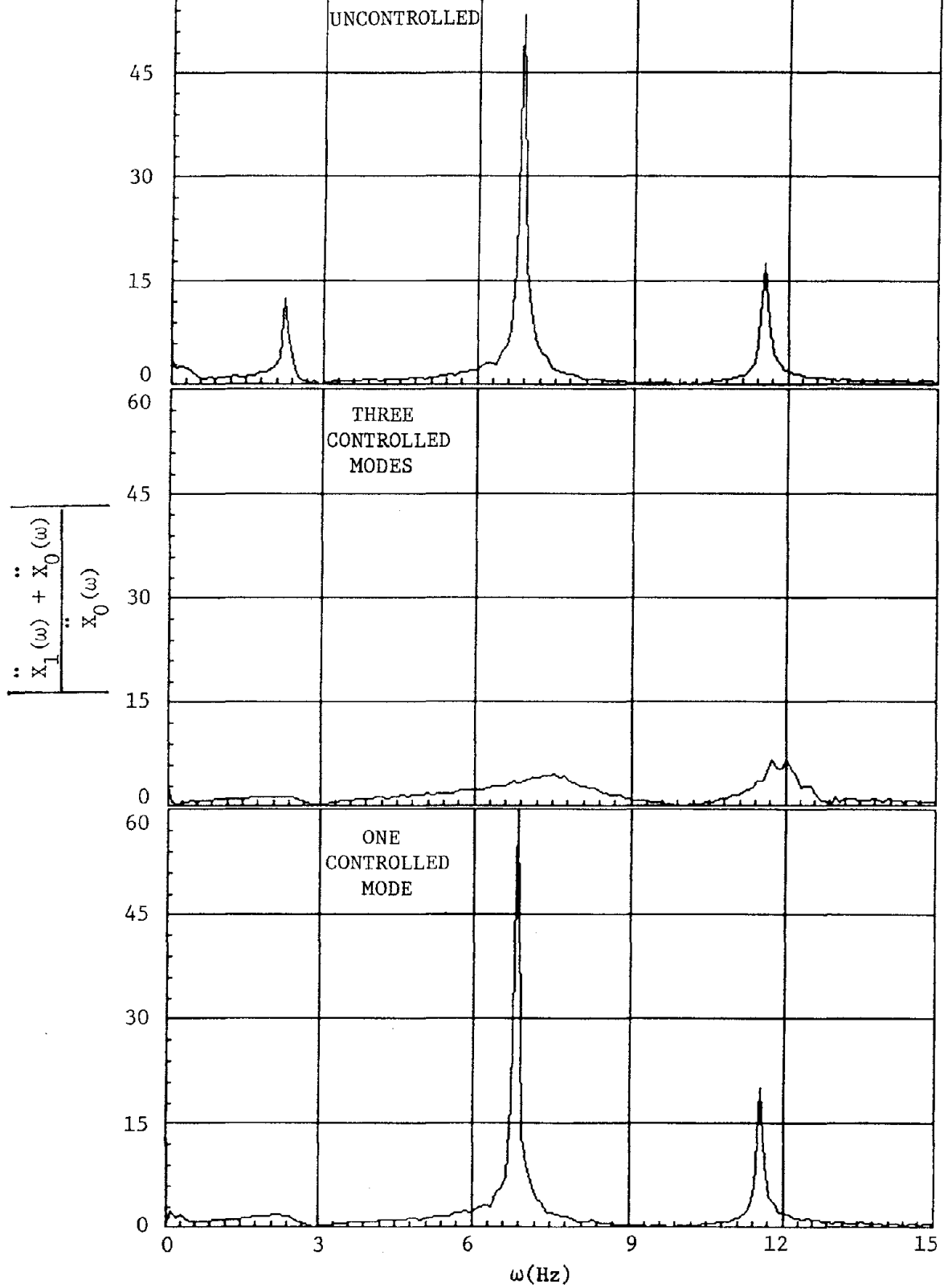
FIGURE 5-5 First-floor Acceleration Frequency Response Functions for the Classical Closed-loop Algorithms

5-10
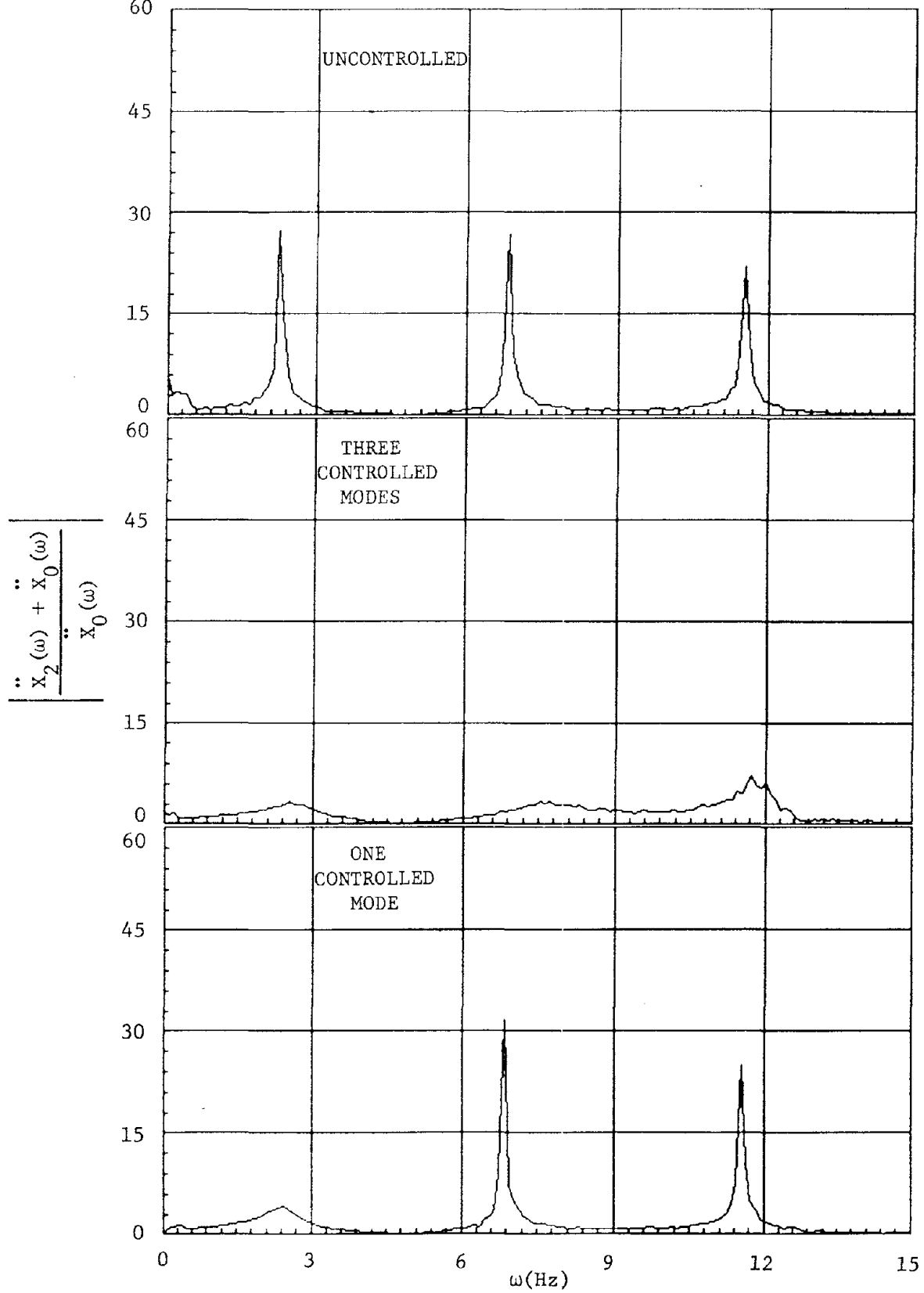
FIGURE 5-6 Second-floor Acceleration Frequency Response Functions for the Classical Closed-loop Algorithms

5-11
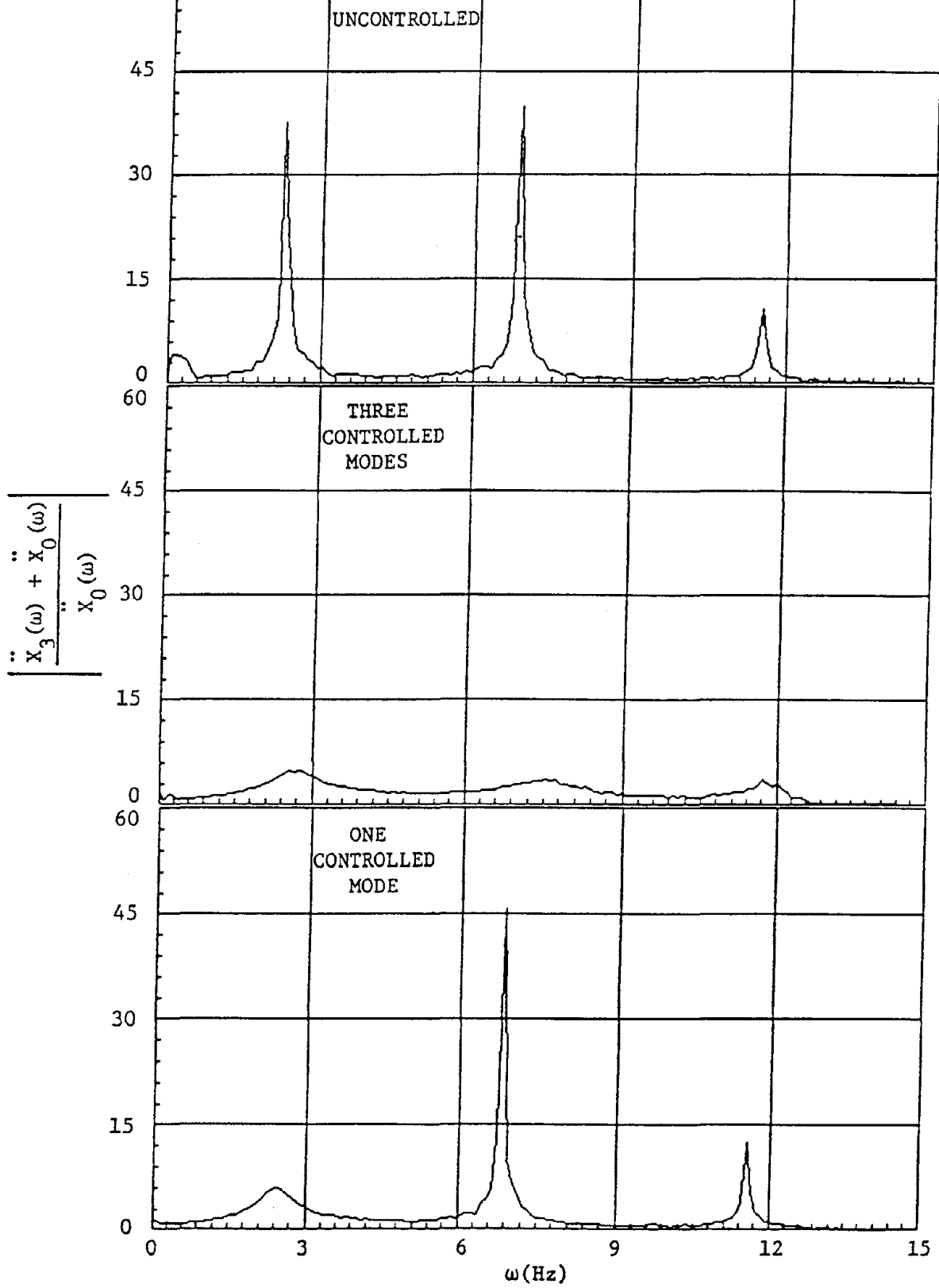
FIGURE 5-7 Third-floor Acceleration Frequency Response Functions for the Classical Closed-loop Algorithms
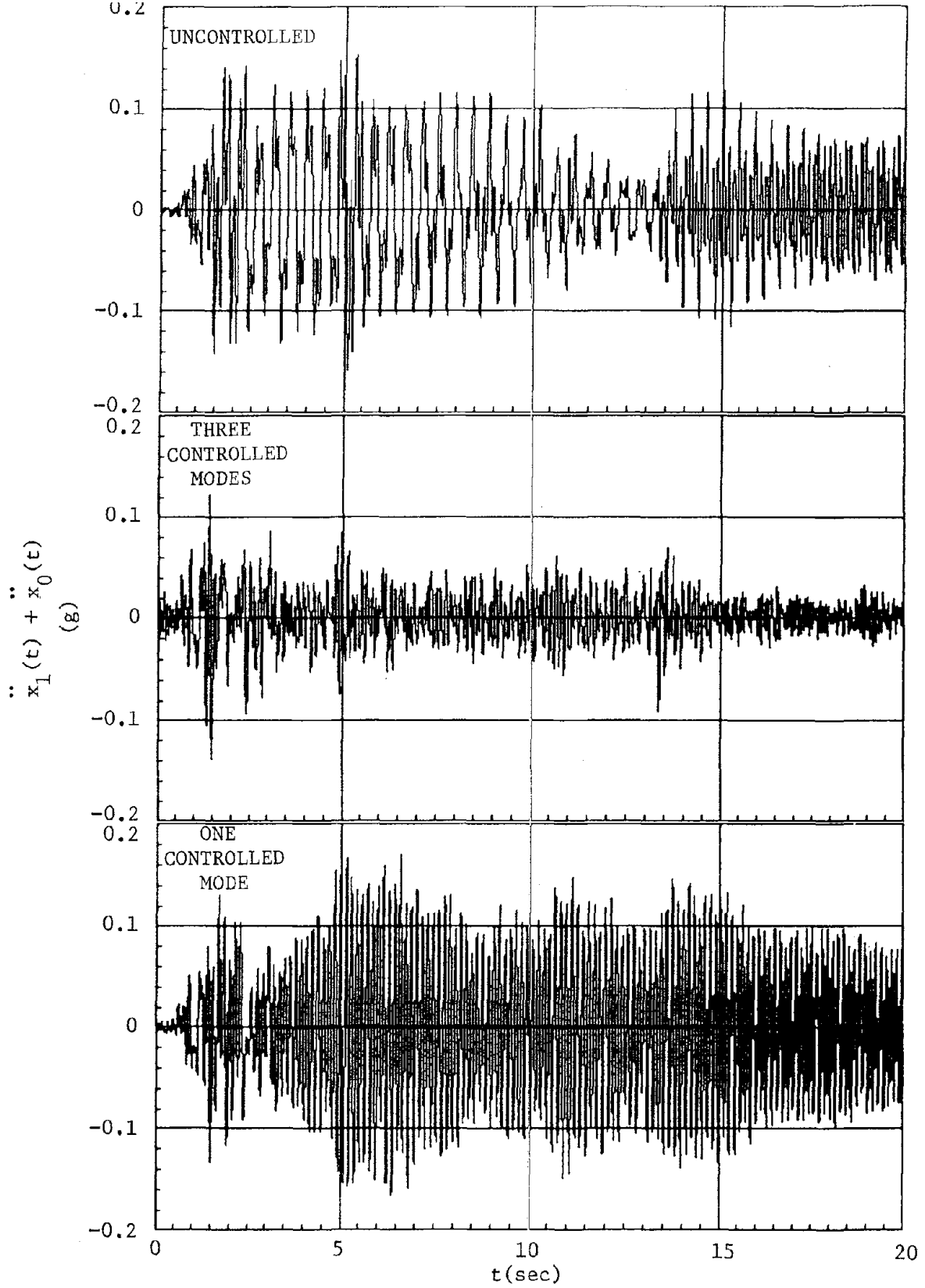
FIGURE 5-8   First-floor Accelerations Under El Centro Excitation for the Classical Closed-loop Algorithms
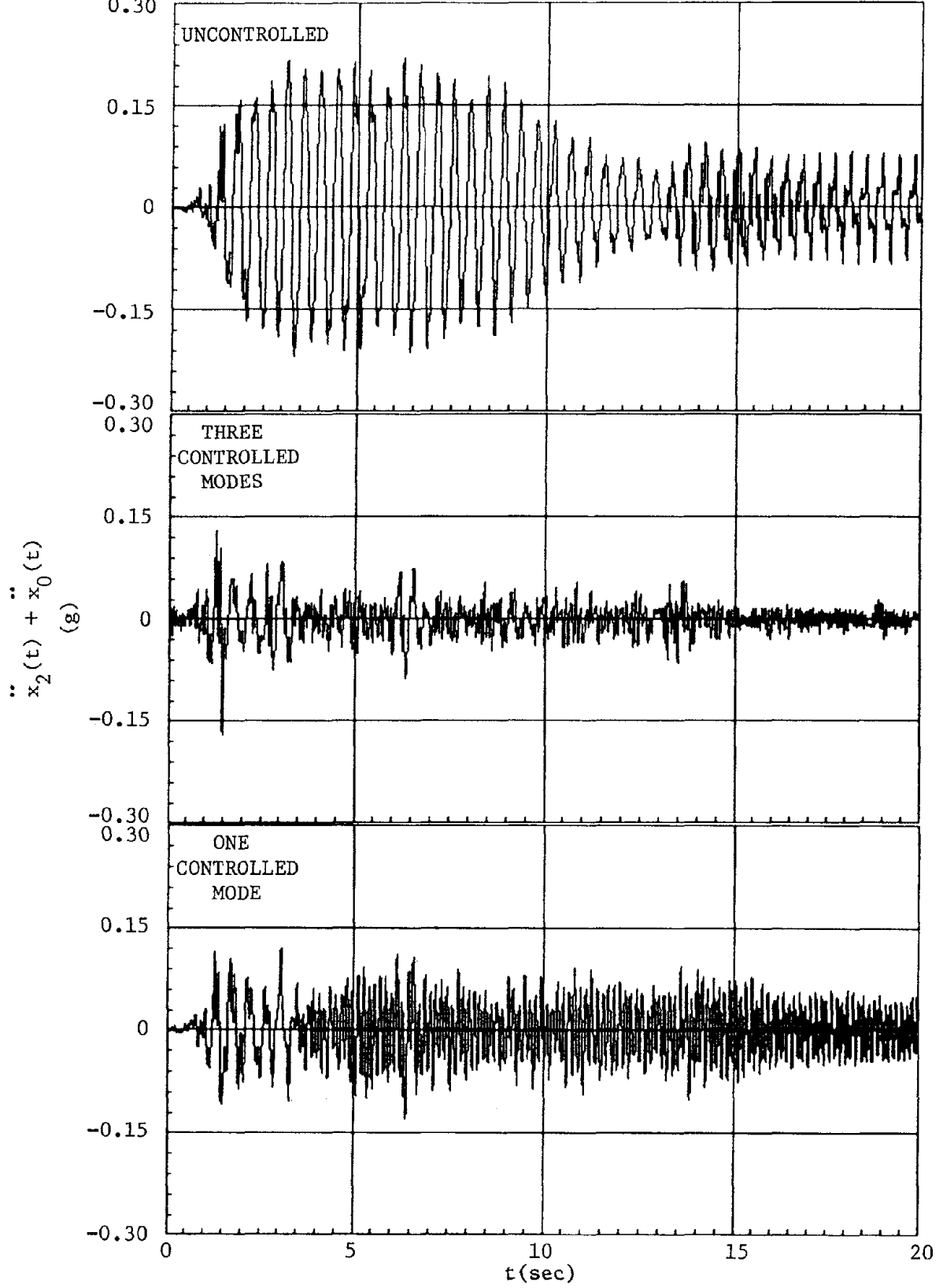
FIGURE 5-9   Second-floor Accelerations Under El Centro Excitation for the
Classical Closed-loop Algorithms

5-14
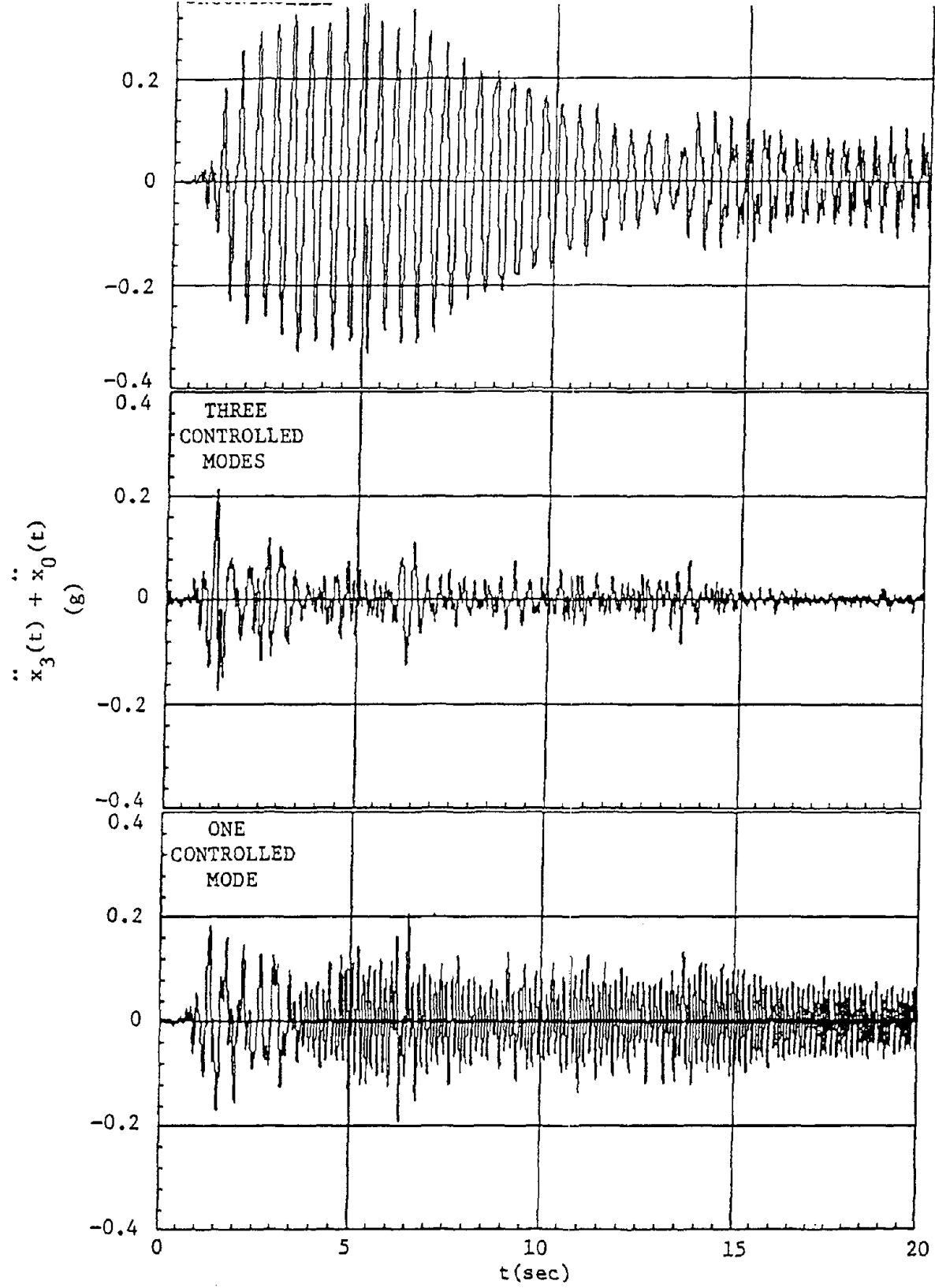
FIGURE 5-10 Third-floor Accelerations Under El Centro Excitation for the Classical Closed-loop Algorithms

5-15

$$
Q = \begin{bmatrix}
Q & & & & & \\
& \beta Q & & & O & \\
& & \beta Q & & & \\
& & & Q & & \\
& O & & & \beta Q & \\
& & & & & \beta Q
\end{bmatrix}
\qquad (5\text{-}1)
$$

where β is a weighting factor. From the derivation of the control algorithms [7], it is known that the control efficiency is dependent on the parameters Q/R and β. Determination of control parameters can be carried out by using computer simulation and these results are shown in Fig. 5-11. From this figure, the suitable control parameters were chosen to be Q/R = 5×10^5 $(in^2/lb^2\text{-}sec^2)$ and $\beta = 0$, but the value of Q/R was subsequently reduced to 5×10^4 $(in^2/lb^2\text{-}sec^2)$ in conducting the actual experiments due to a significant increase in the maximum control force when the value of Q/R was larger than 5×10^4 $(in^2/lb^2\text{-}sec^2)$. A set of typical experimental results are shown in Fig. 5-12 through 5-18.

The maximum response values measured during the experimental study, along with reduction produced by the active control compared to the uncontrolled case, are shown in Table 5-3. The average reductions (control efficiencies) are only 27%-36% due to the use of only one controller in this study. The closed-loop control is slightly more efficient than the others, close to open-closed loop performance. All three algorithms proved to be feasible to implement for response reduction.

During these tests several methods of time delay compensation [10] were studied. Only the method of 'phase shift' presented in this paper was successful in the control of the three-story system.

5.4 EXPERIMENTAL VS ANALYTICAL RESULTS

Good agreement was achieved between analytical and experimental results (Figs. 5-19 through 5-22). The discrepancies were larger in the

TABLE 5-III   Comparison of the Instantaneous Optimal Control Algorithms
(Experimental Results)

Control Algorithms	FLOOR	Relative Displacement			Storydrift Displacement			Absolute Acceleration			$|u(t)|_{max}$ Weight
		Value	Red.	Effi.	Value	Red.	Effi.	Value	Red.	Effi.	
		in.	%	%	in.	%	%	g	%	%	%
Uncontrol	1	0.2134			0.2134			0.1576			
	2	0.4594			0.2621			0.2210			
	3	0.6323			0.1787			0.3223			
Open-loop Control	1	0.1444	33.3		0.1444	33.3		0.1156	26.6		
	2	0.3324	27.6	29.3	0.1952	25.5	28.7	0.1605	27.4	26.8	2.20
	3	0.4623	26.9		0.1299	27.4		0.2373	26.4		
Open-closed-loop Control	1	0.1370	35.8		0.1370	35.8		0.1146	27.3		
	2	0.2898	36.9	36.2	0.1694	35.4	35.4	0.1576	28.6	29.9	3.84
	3	0.4060	35.8		0.1162	35.0		0.2129	33.9		
Closed-loop Control	1	0.1255	41.2		0.1255	41.2		0.0990	37.2		
	2	0.2978	35.2	36.7	0.1777	32.2	35.1	0.1468	33.6	33.6	2.88
	3	0.4189	33.7		0.1216	32.0		0.2256	30.0		

NOTES:

Red = $1 - R_{con}/R_{unc}$ is the response reduction where R_{con} is the controlled response and R_{unc} is the uncontrolled response.

$\overline{Effi}$ is the efficiency average based on average reduction.

$|u(t)|_{max}$ is the maximum control force.
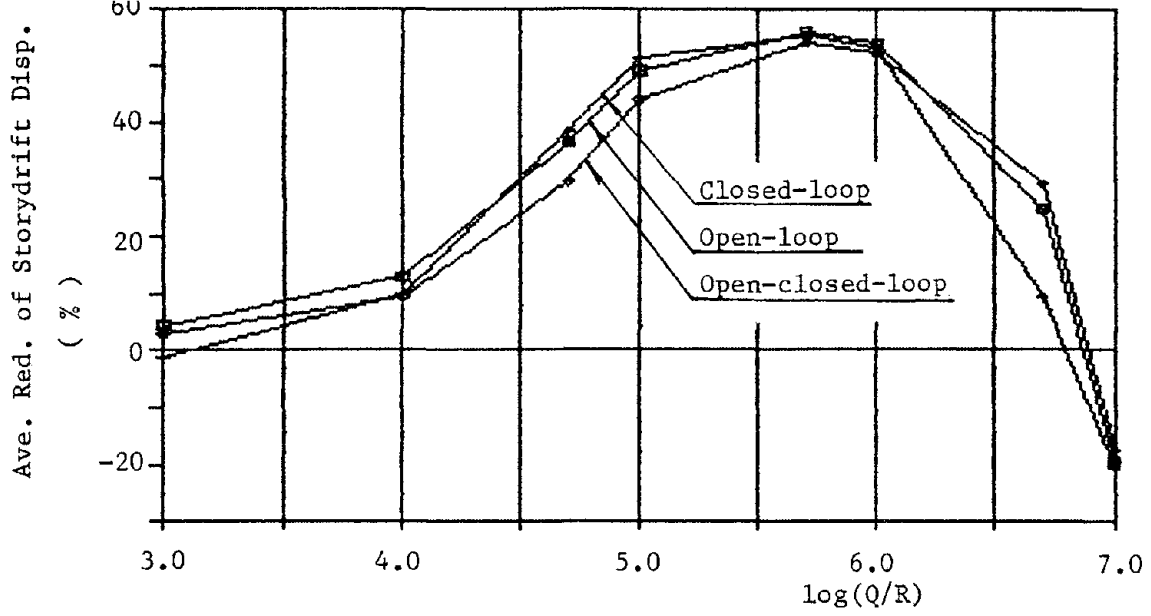
a) Control Efficiency Based on (Q/R) under $\beta = 0$
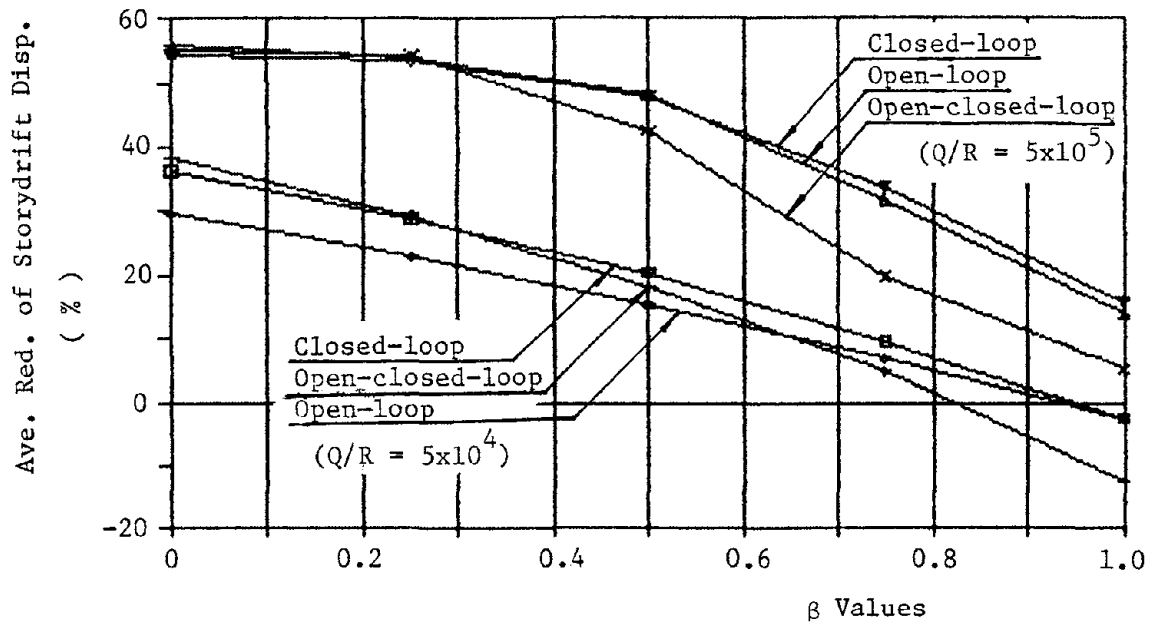
b) Control Efficiency Based on β Values

FIGURE 5-11   Comparisons of Control Parameters for Instantaneous Optimal
Algorithms
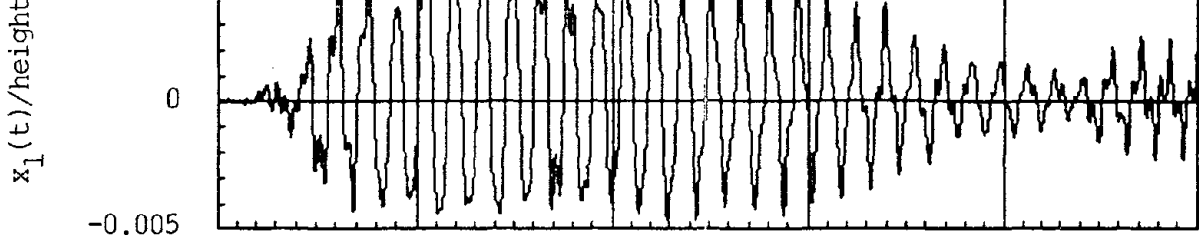
a) Uncontrolled
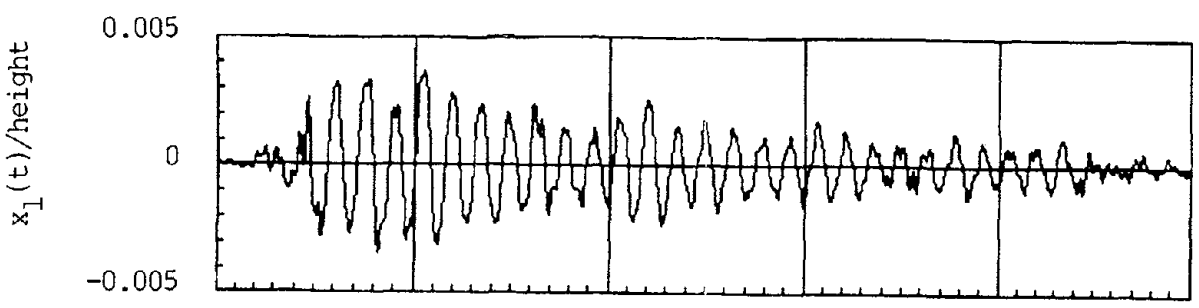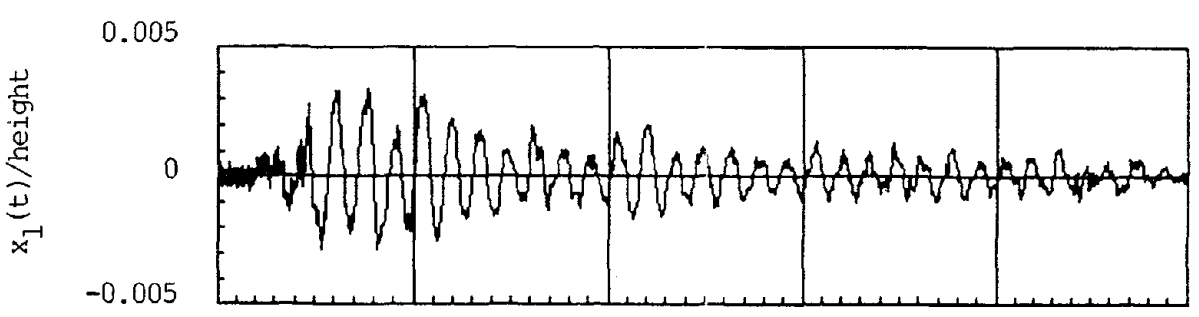
b) Open-loop Control

c) Open-closed-loop Control
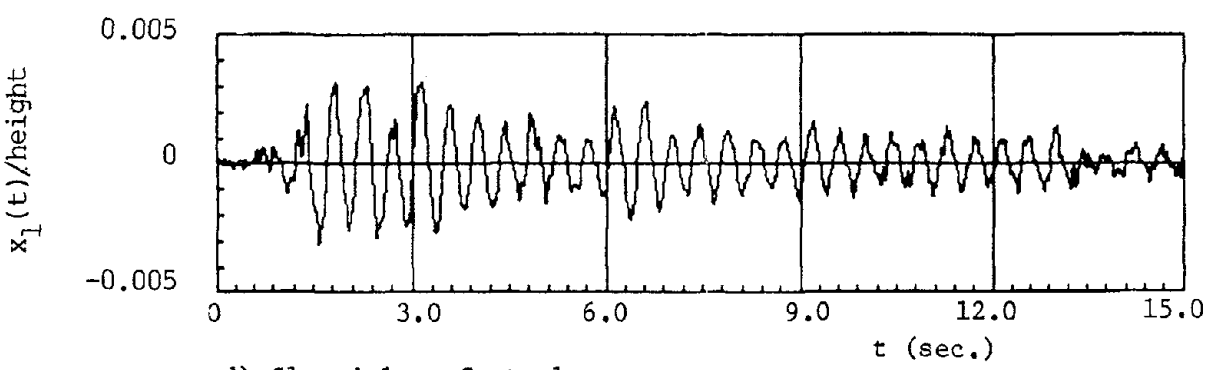
d) Closed-loop Control

FIGURE 5-12 Relative Displacement Response of First-Floor for Instantaneous Optimal Control Algorithms
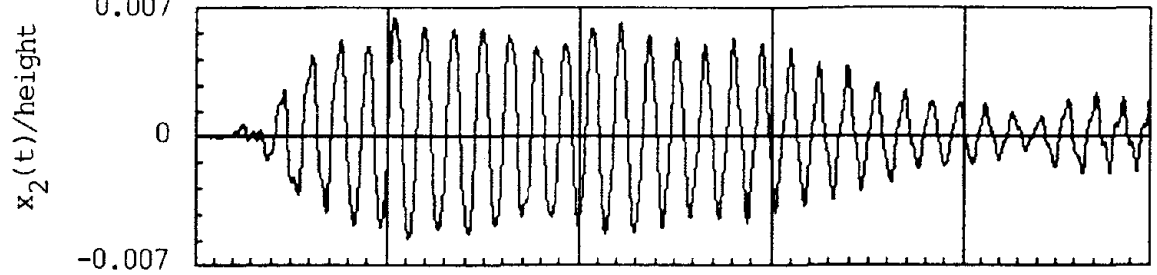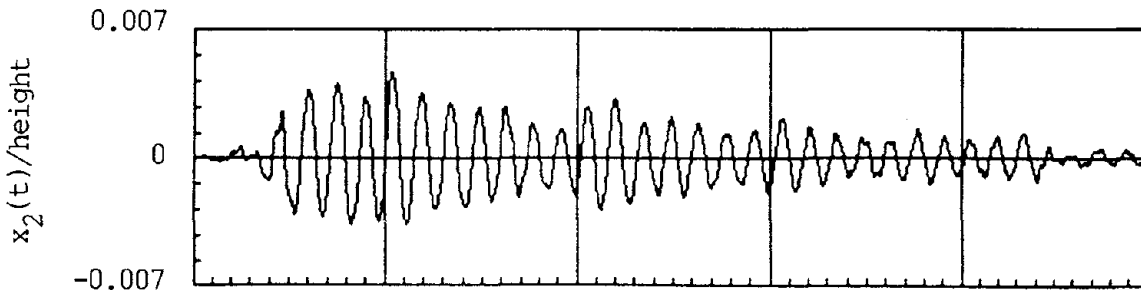
a) Uncontrolled
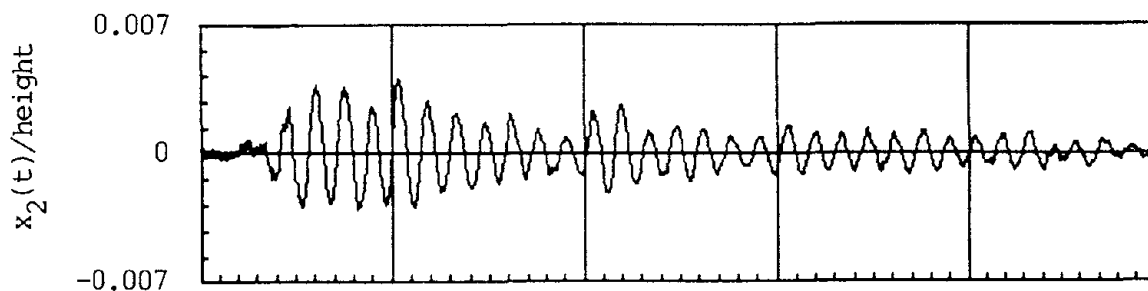
b) Open-loop Control

c) Open-closed-loop Control
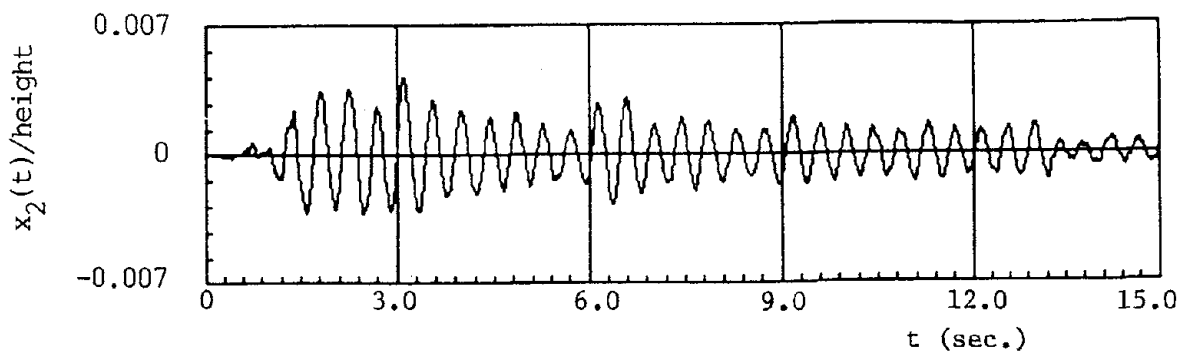
d) Closed-loop Control

FIGURE 5-13 Relative Displacement Response of Second-Floor for Instantaneous
Optimal Control Algorithms
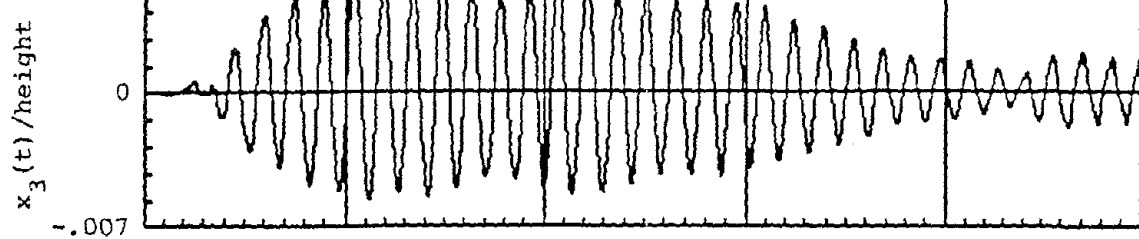
a) Uncontrolled
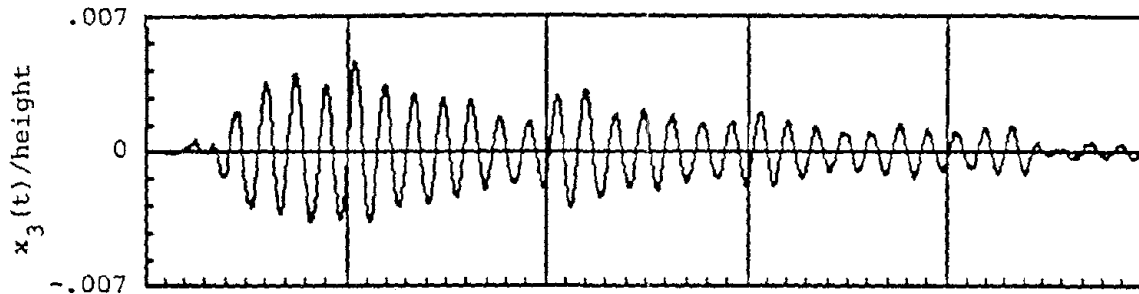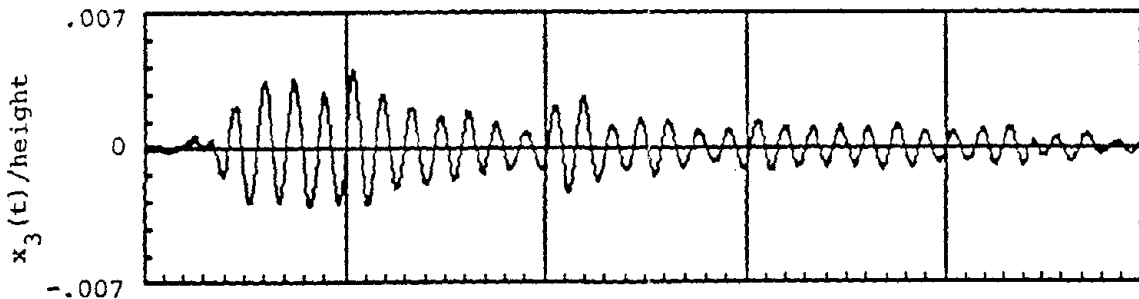
b) Open-loop Control

c) Open-Closed-loop Control
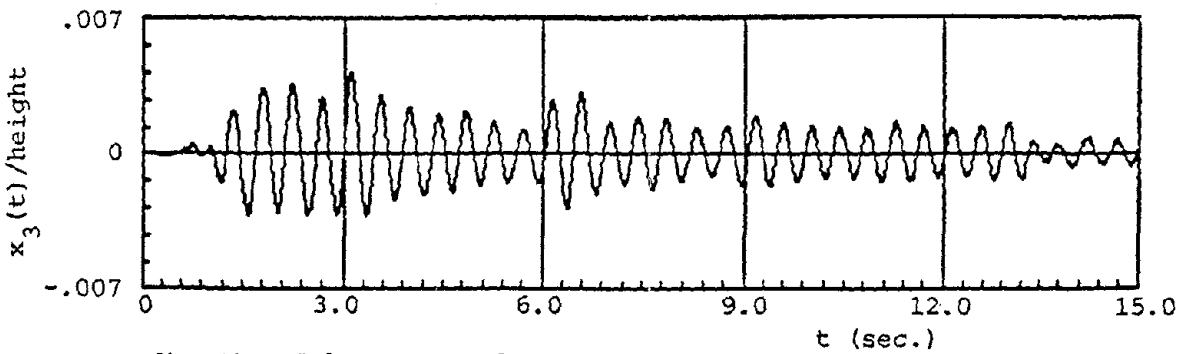
d) Closed-loop Control

FIGURE 5-14   Relative Displacement Response of Third-Floor for Instantaneous
Optimal Control Algorithms

5-21

a) Uncontrolled

b) Under Instantaneous Open-closed-loop Control
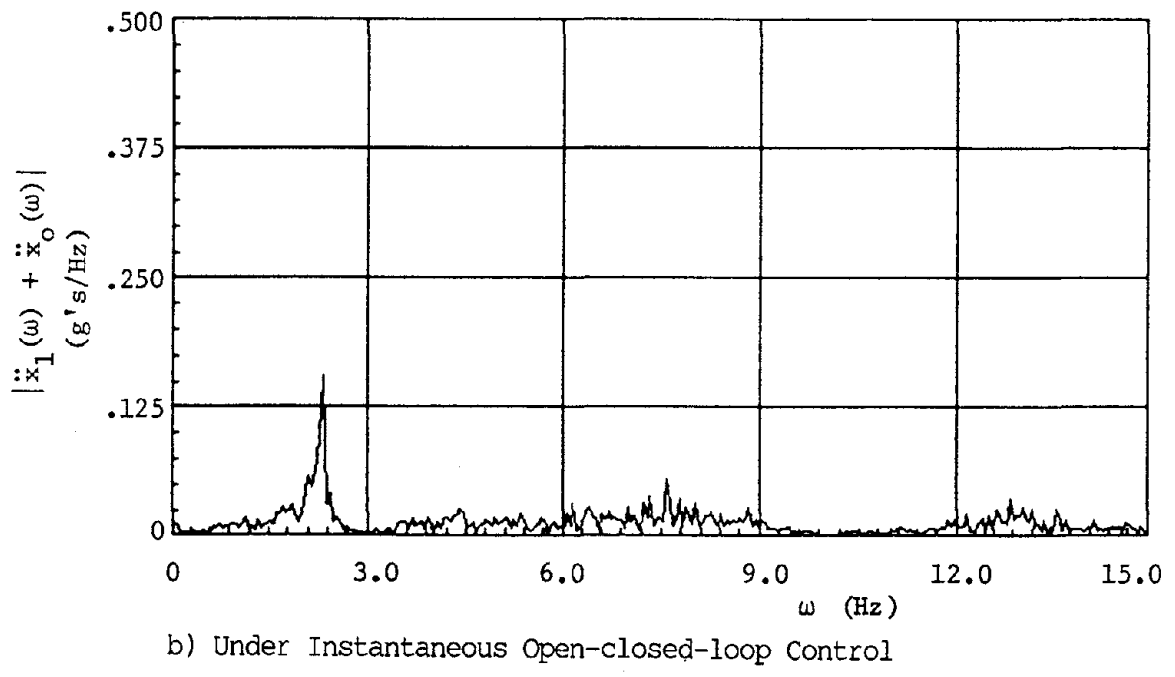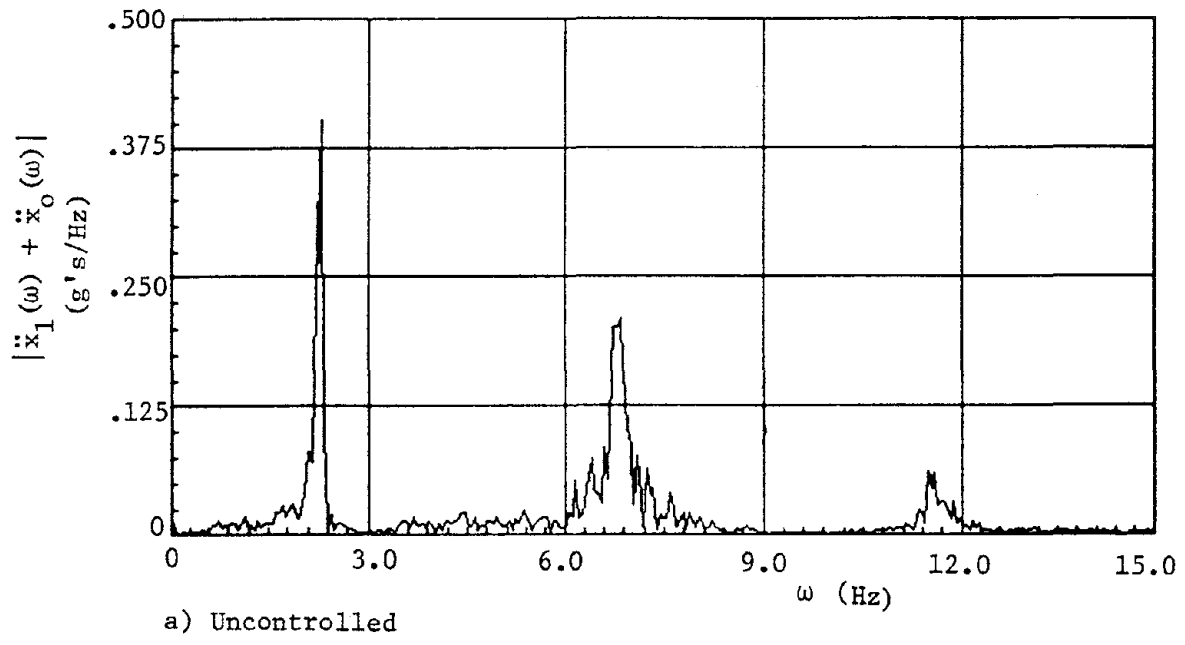
FIGURE 5-15 First-Floor Acceleration Frequency Response

5-22

a) Uncontrolled

b) Under Instantaneous Open-closed-loop Control
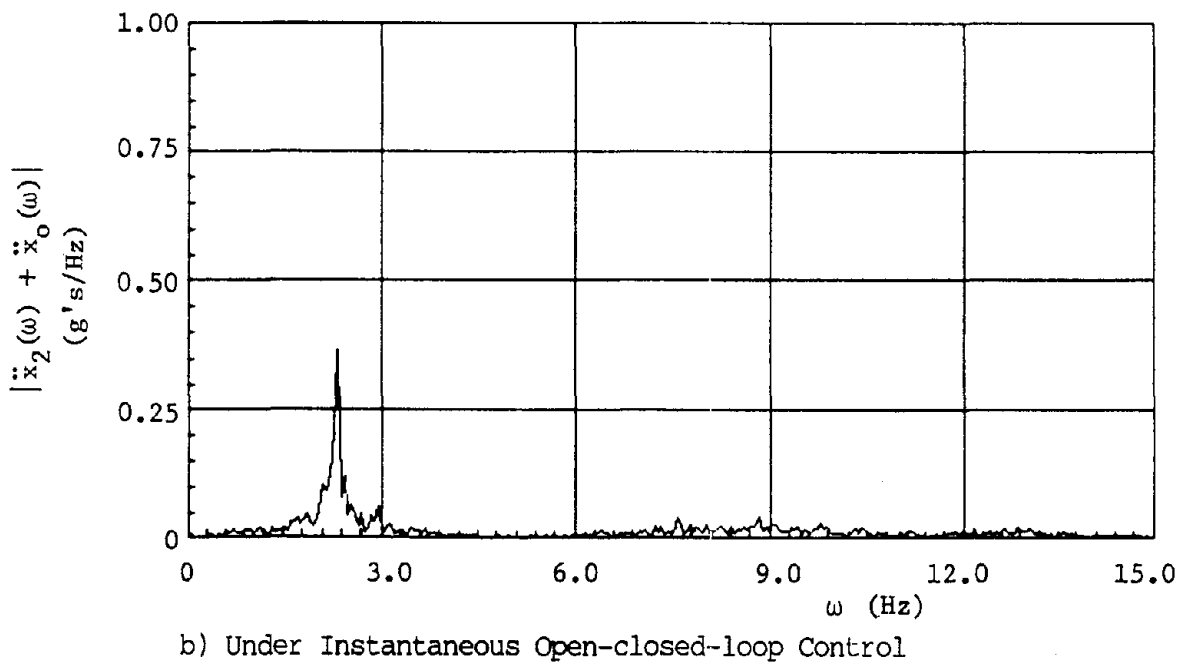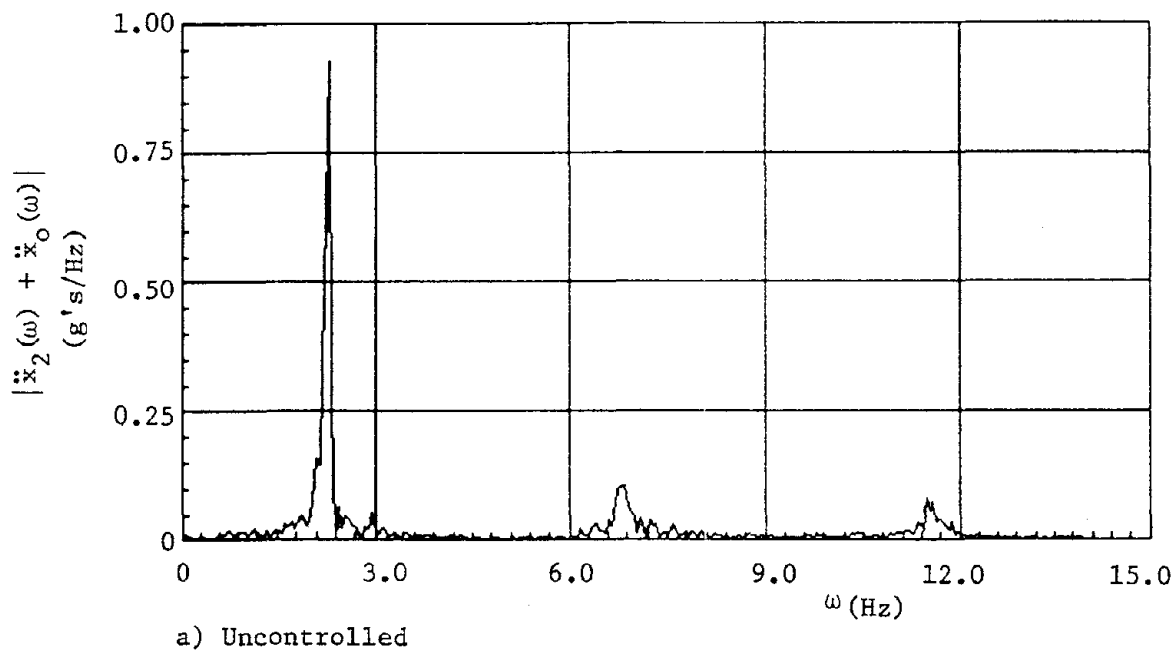
FIGURE 5-16 Second-Floor Acceleration Frequency Response

a) Uncontrolled

b) Under Instantaneous Open-closed-locp Control
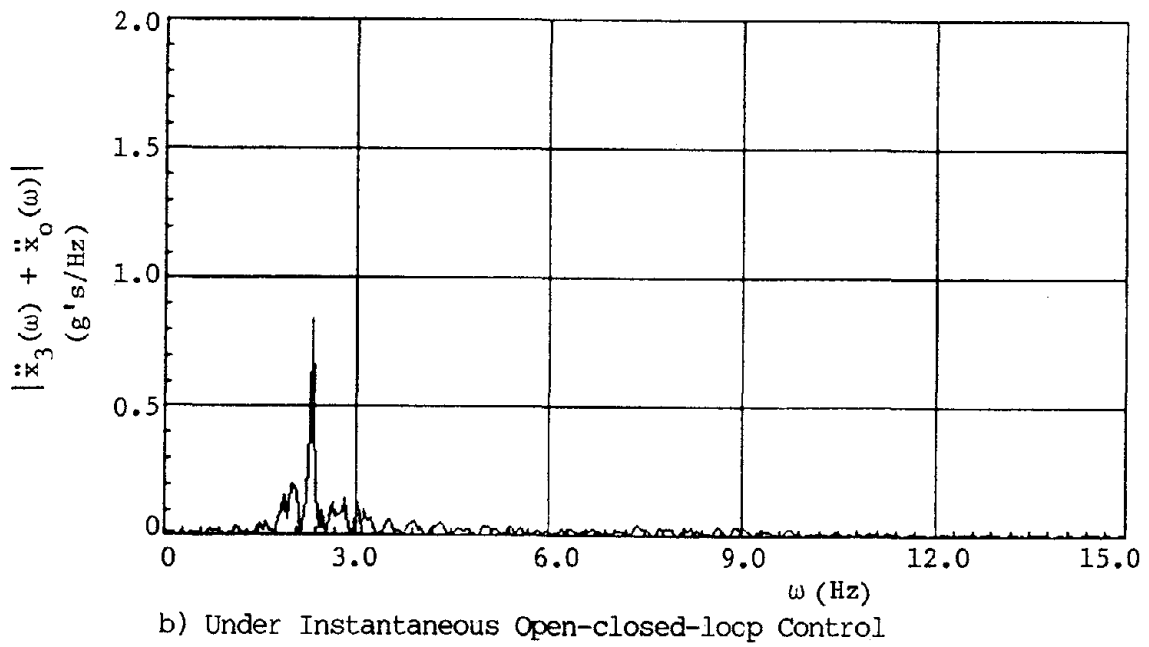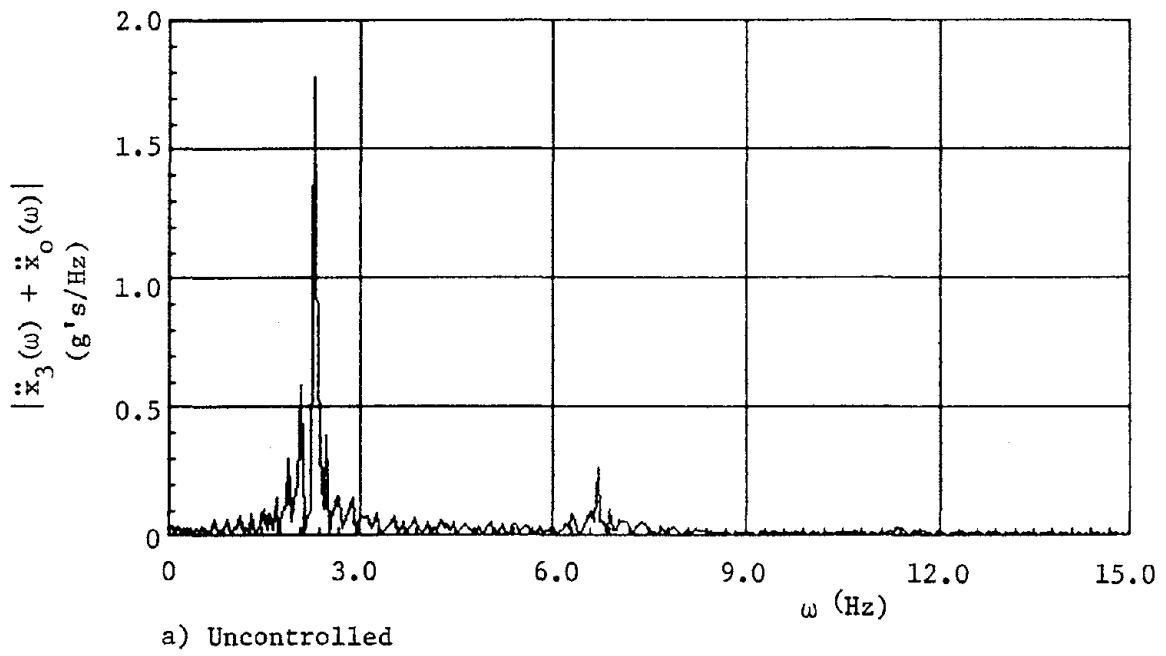
FIGURE 5-17   Third-Floor Acceleration Frequency Response

5-24
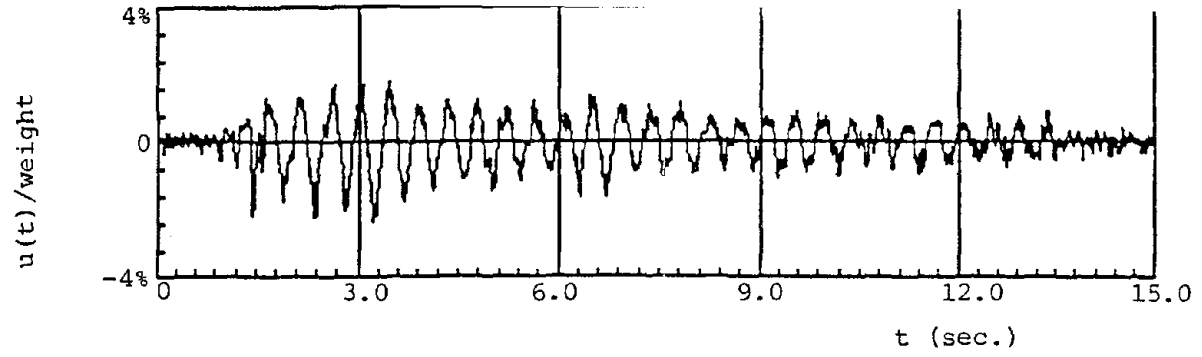
a) Open-loop Control
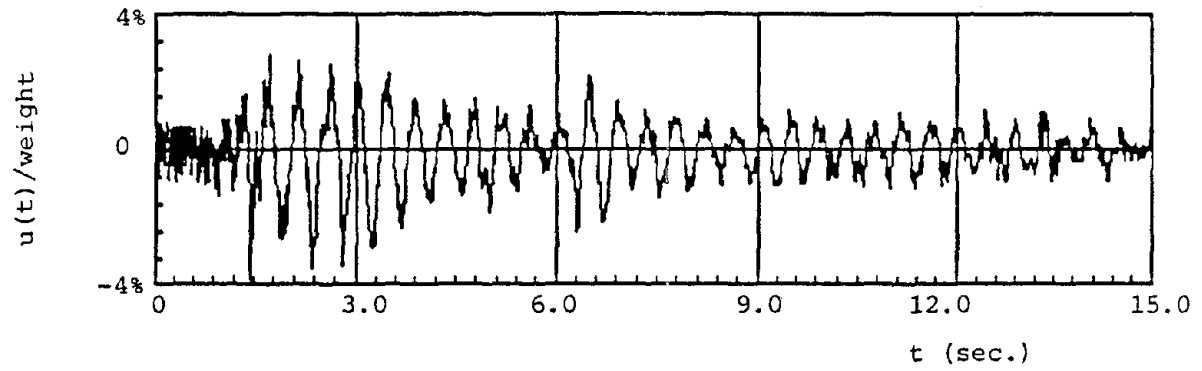
b)   Open-closed-loop Control
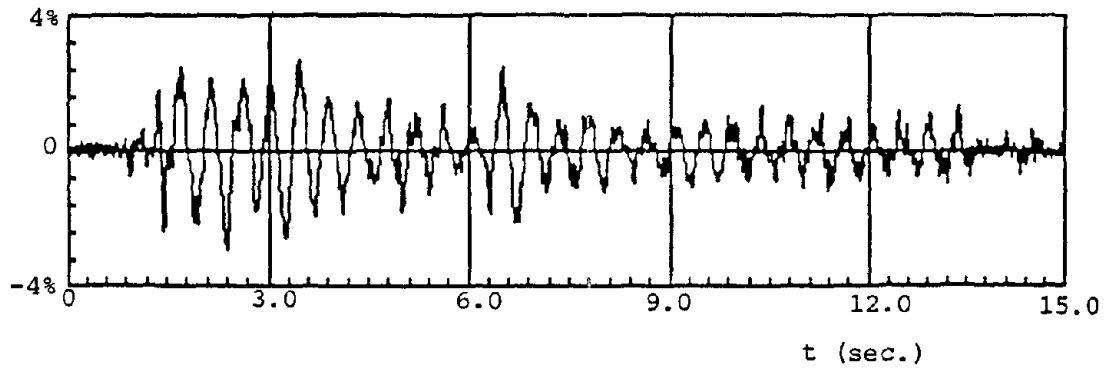
c)   Closed-loop Control

FIGURE 5-18   Time History of Control Forces for Instantaneous Optimal Control
Algorithms

5-25
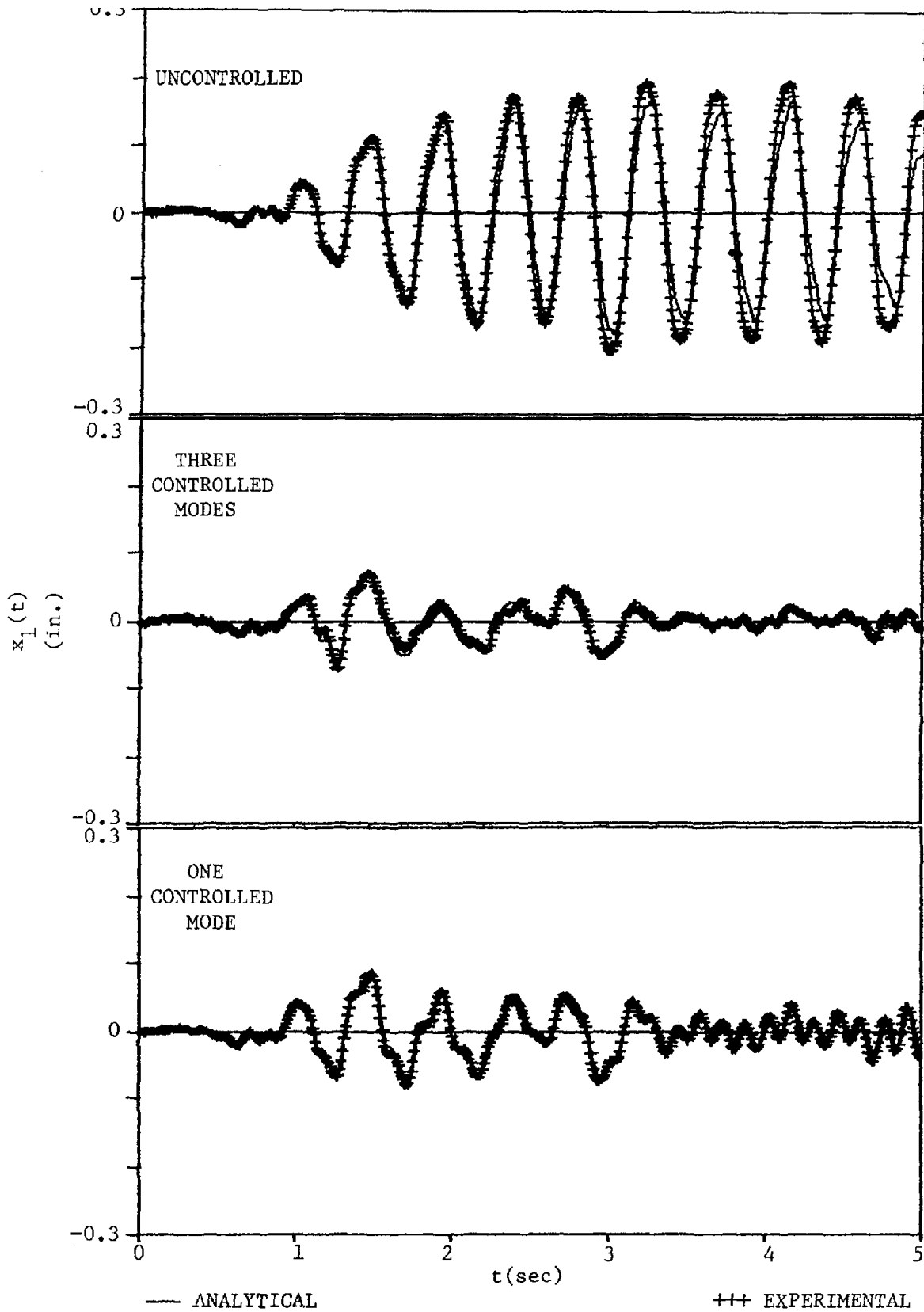
FIGURE 5-19 First-floor Relative Displacements Under El Centro Excitation for the Classical Closed-loop Algorithms
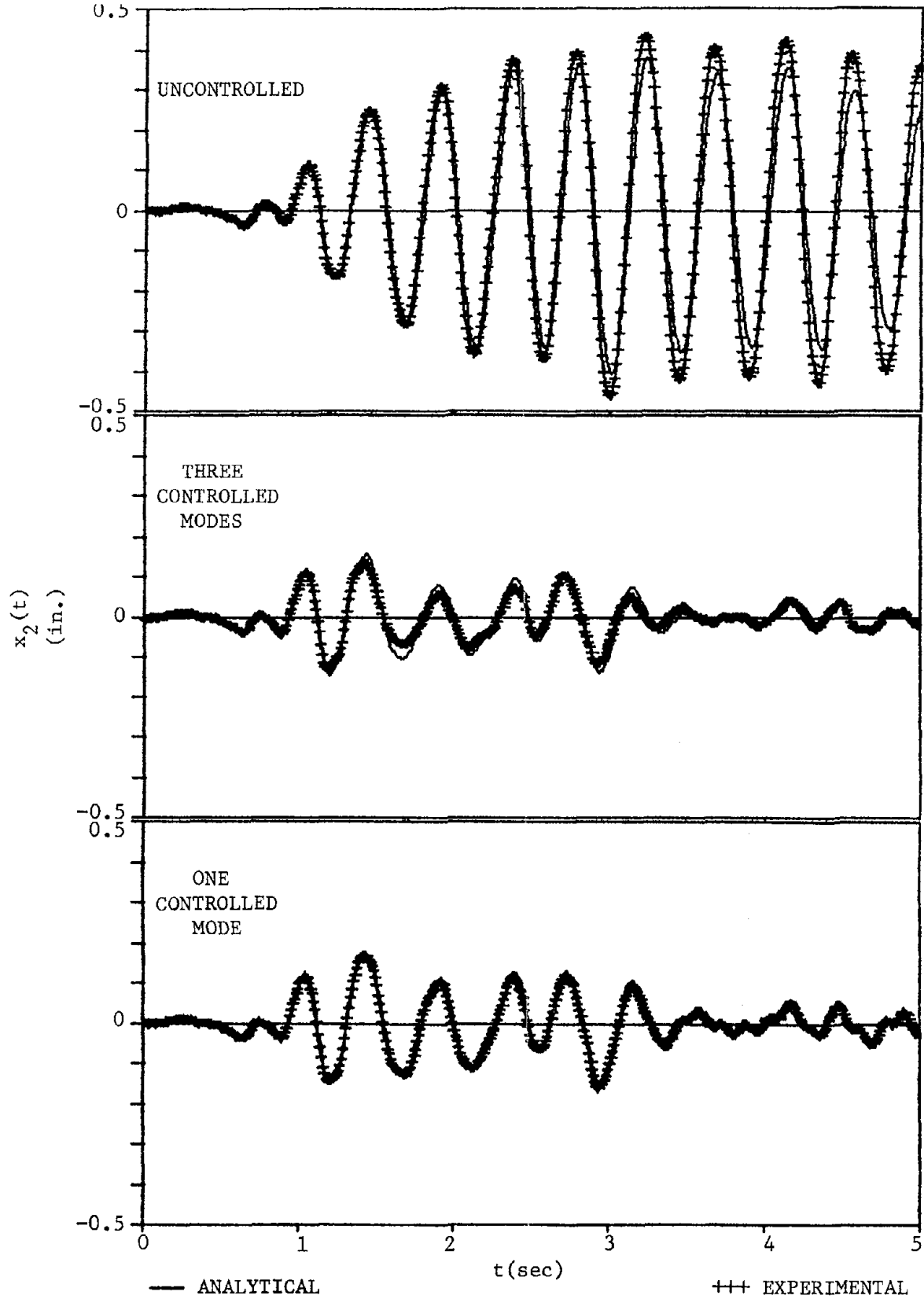
FIGURE 5-20 Second-floor Relative Displacements Under El Centro Excitation
for the Classical Closed-loop Algorithms

5-27
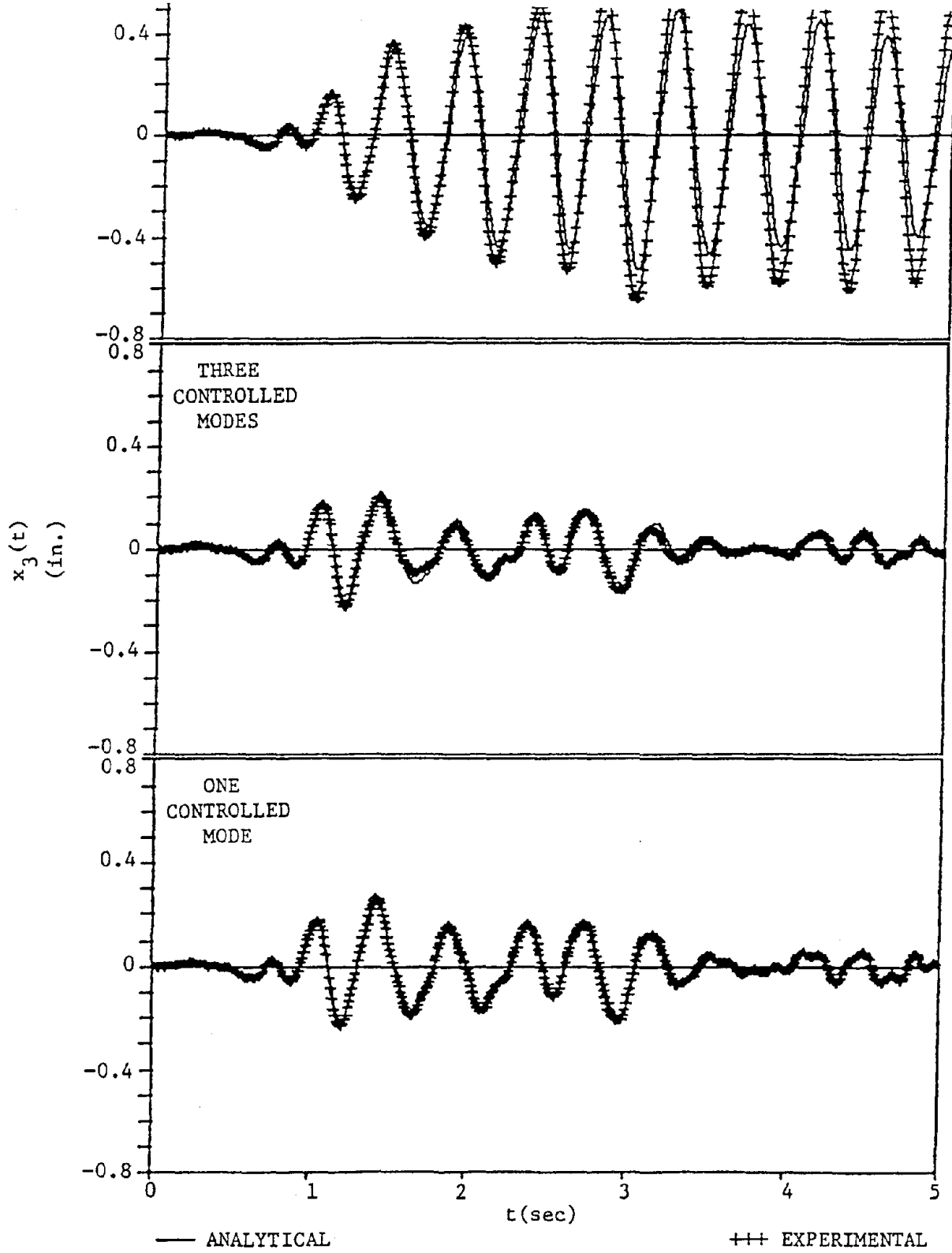
FIGURE 5-21   Third-floor Relative Displacements Under El Centro Excitation for the Classical Closed-loop Algorithms
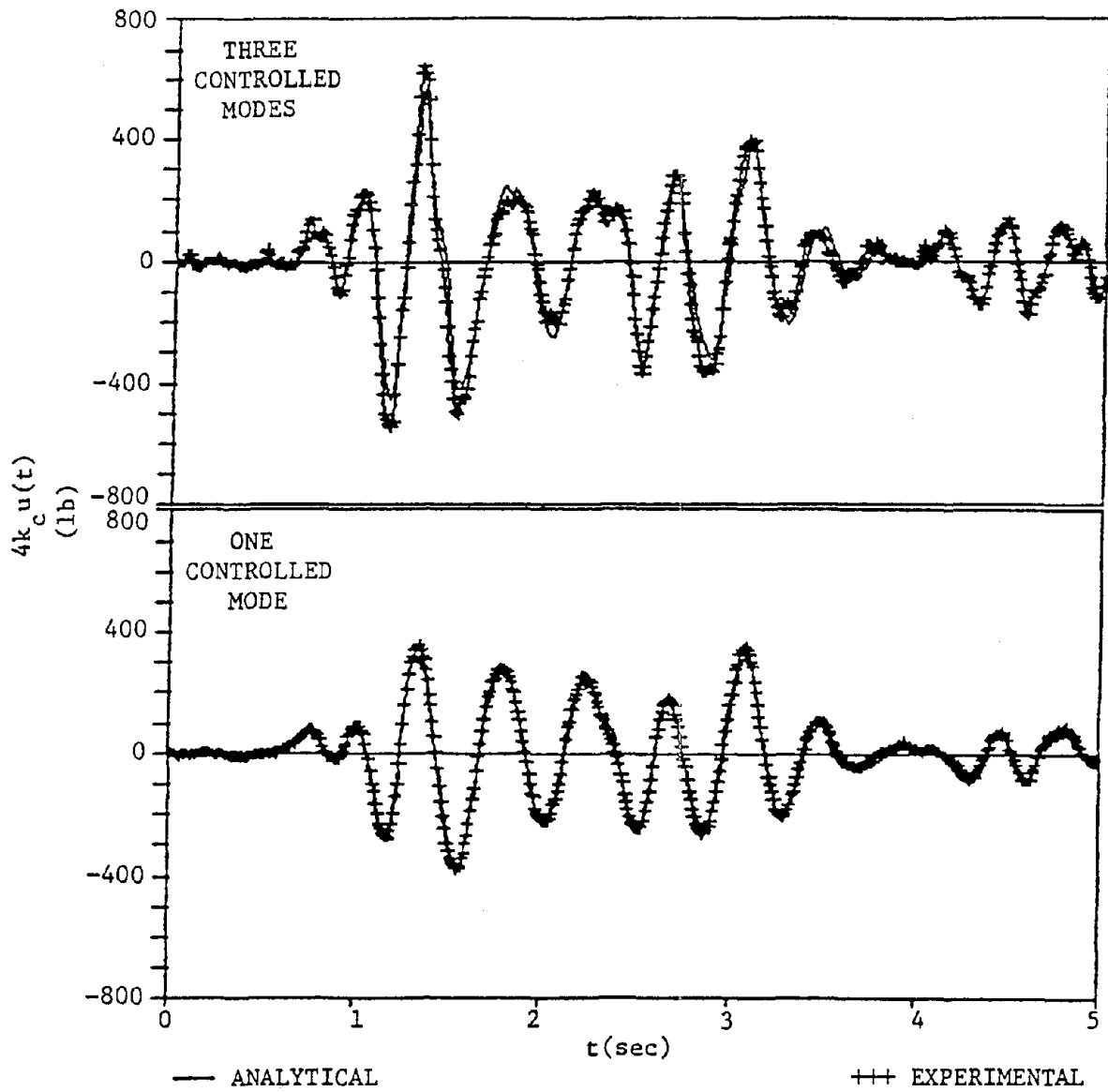
FIGURE 5-22   Control Forces Under El Centro Excitation for the Classical Closed-loop Algorithms

uncontrolled test due to the servo-controlled system. The actuator was kept stationary by this system during uncontrolled tests. However, slight actuator movement was induced by the structural motion and the actuator movement was continuously corrected to reduce the error to zero. This interaction between the controller and the structure made the damping force a complicated function of the structural response. For the case of El Centro excitation, some discrepancies resulted from the fact that the equivalent viscous damping was different from the calibrated one measured in the banded white noise tests. However, for the controlled cases, most of the damping force was contributed by the feedback force. Therefore, the influence of actuator-structure interaction was negligible and excellent agreement was observed. With one controlled mode, the control force was of a lower magnitude and of a lower frequency, leading to a better performance of the actuator and hence excellent agreement was achieved.

The comparisons of experimental results of instantaneous algorithms and the analytical results were made. A set of typical results are shown in Figs. 5-23 through 5-26. Details of these studies can be found in [7]. Some discrepancies in the peak values could be noticed with a regular pattern. The analytical results were always smaller than the experimental results. This was caused by the differences between the equivalent viscous damping versus the calibrated value and by the difference in the digitization rates for the input motion during the experiments and analytical studies.
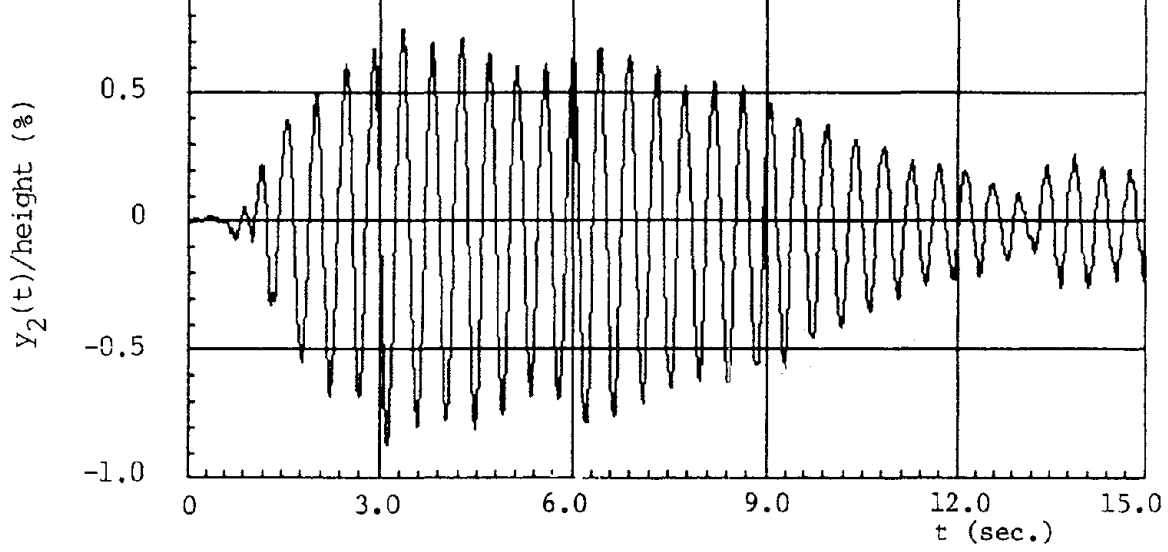
a) Experimental
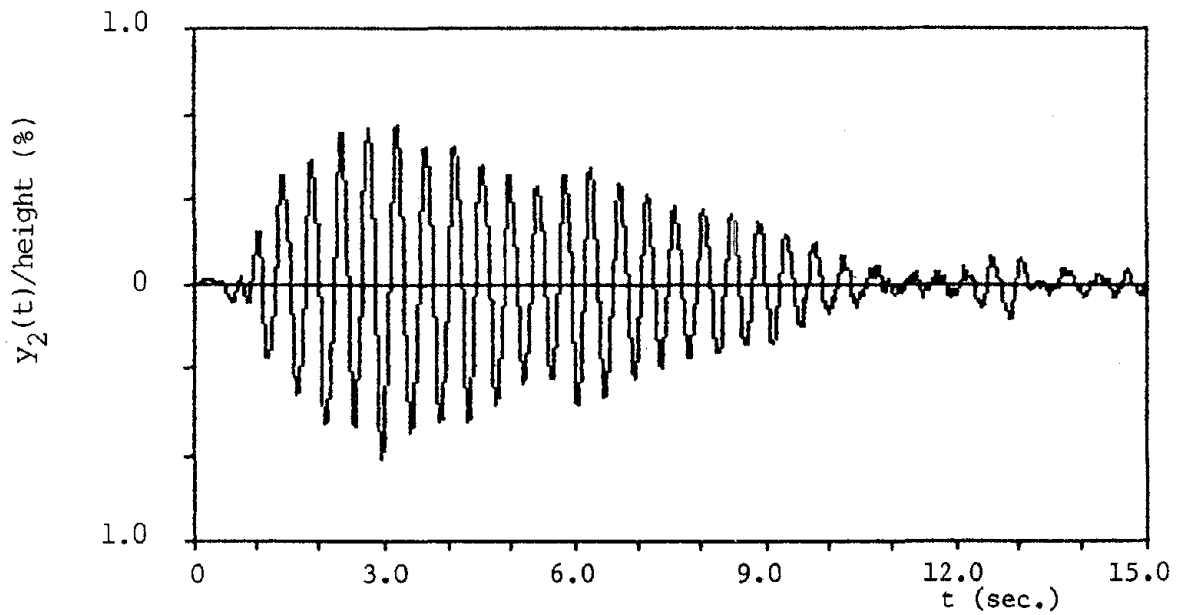
b) Analytical

FIGURE 5-23 Storydrift Displacement Between First and Second Floor in
Uncontrolled Case

5-31

a) Experimental

b) Analytical
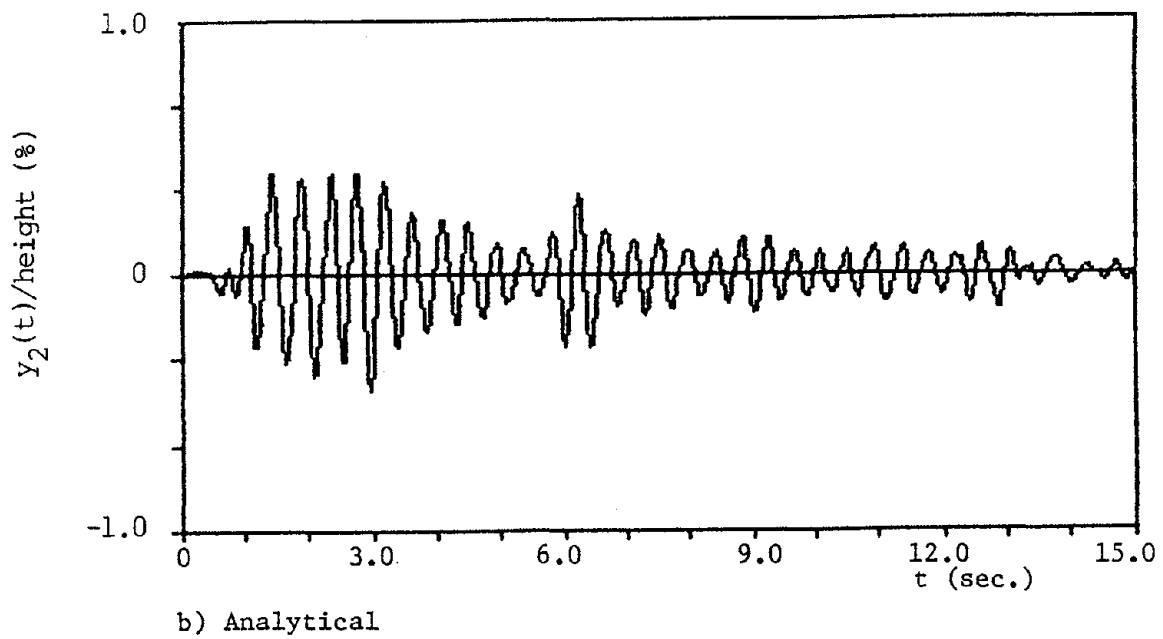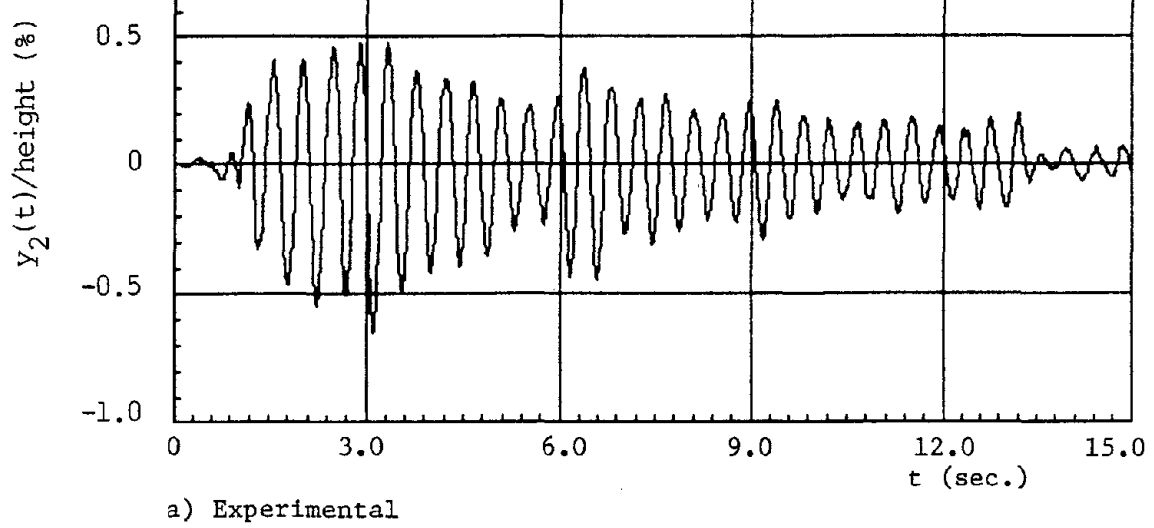
FIGURE 5-24 Storydrift Displacement Between First and Second Floor in
Instantaneous Open-loop Control

a) Experimental

b) Analytical
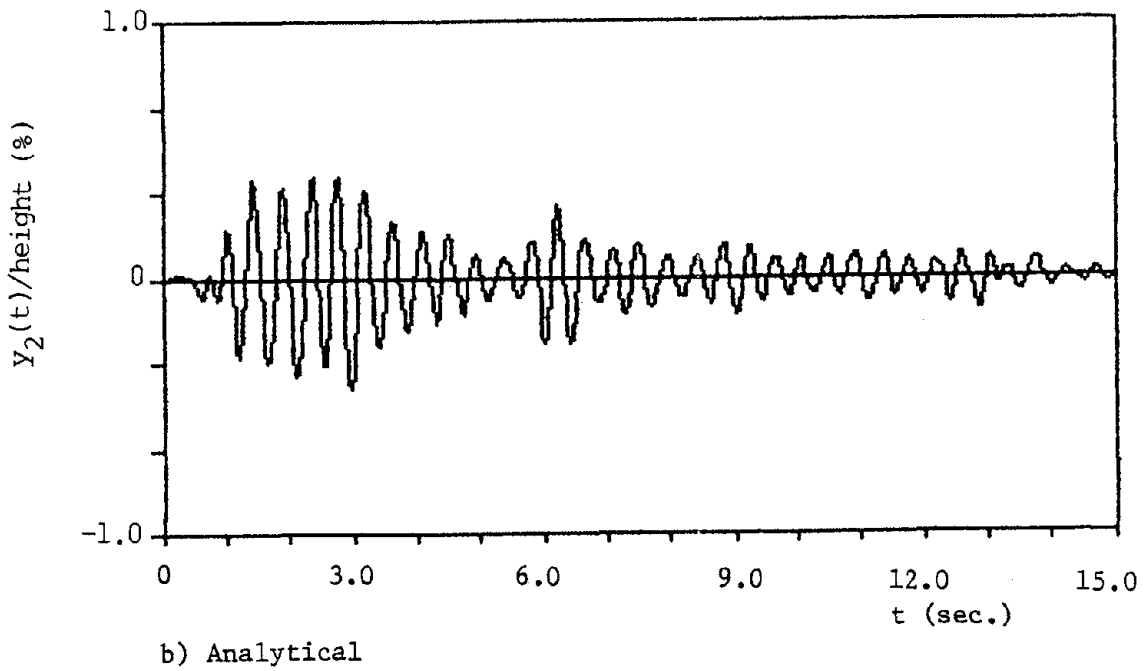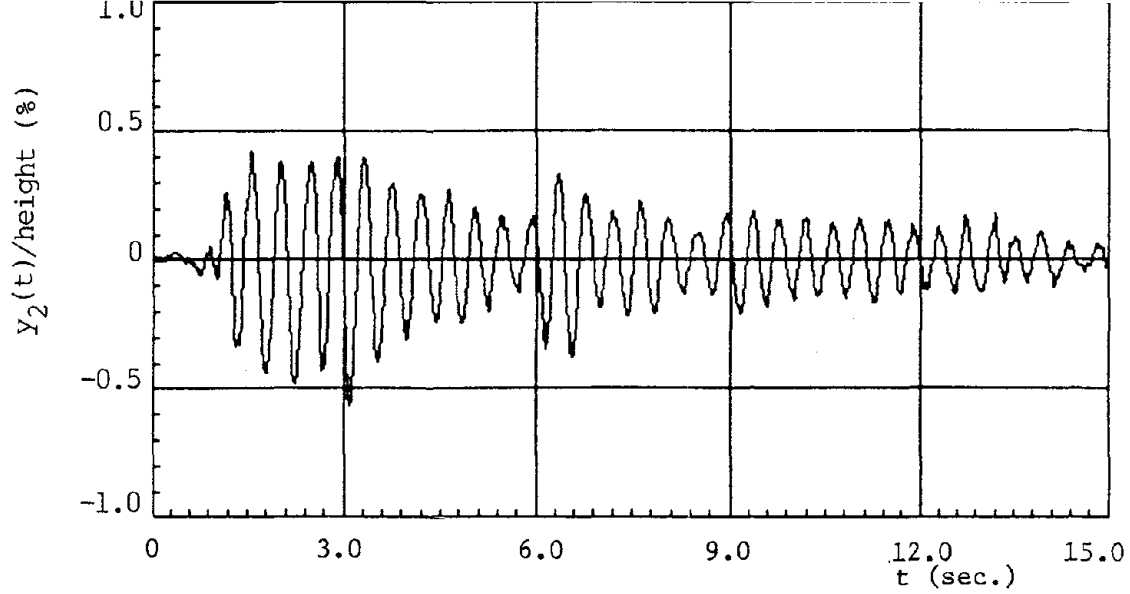
FIGURE 5-25   Storydrift Displacement Between First and Second Floor in
Instantaneous Open-closed-loop Control

5-33

a) Experimental

b) Analytical
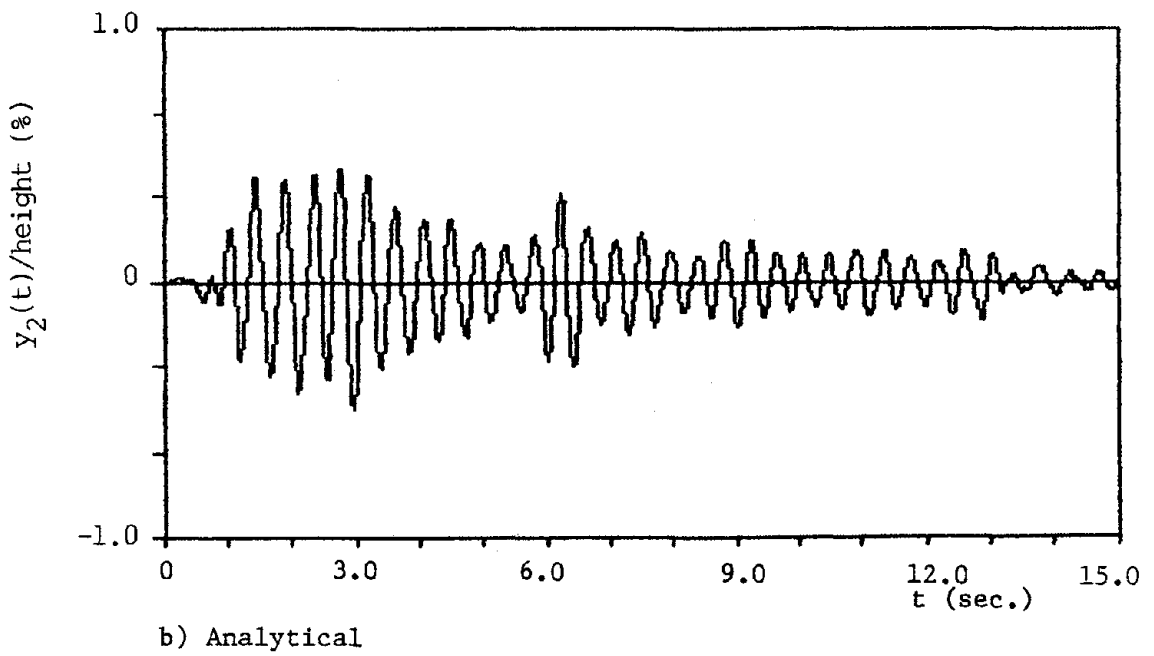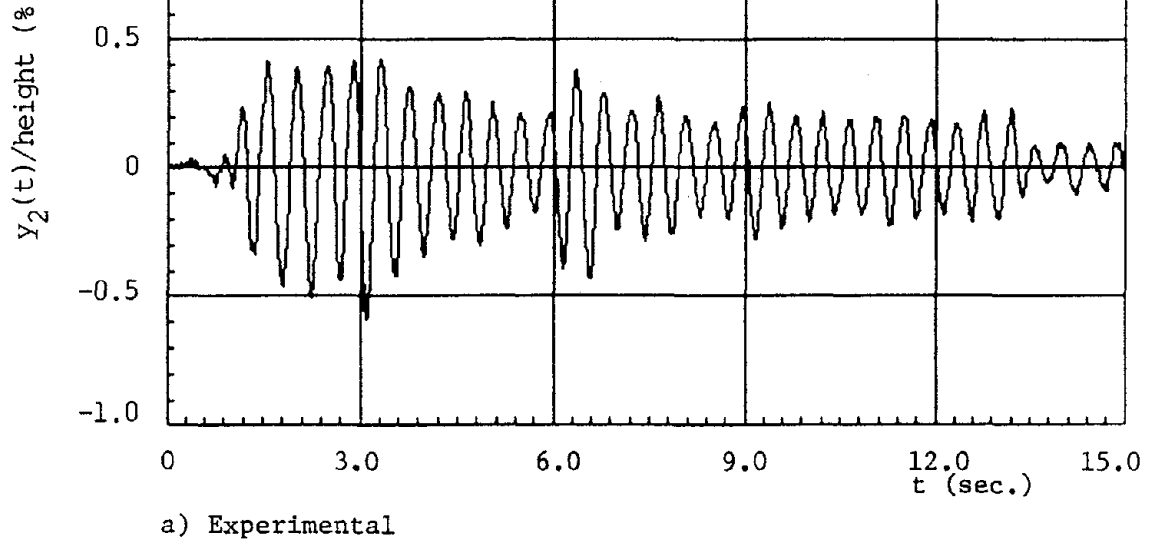
FIGURE 5-26   Storydrift Displacement Between First and Second Floor in
Instantaneous Closed-loop Control

5-34

SECTION 6

DISCUSSIONS AND CONCLUSIONS

Experiments of active control of a three-story building structure with one controller have been carried out successfully under realistic conditions.

In the case of instantaneous optimal open-loop control, it has been shown that, since the control forces were only regulated by the base excitation, time delay compensation was difficult and significant errors were introduced and accumulated in the entire control process. To insure its success, actual measurements of the state variables were necessary and therefore a modification of the original algorithms was made.

For the time delay compensation, three methods were studied after their feasibility was verified experimentally for a SDOF system [10]. In MDOF systems, however, two of the methods, i.e., the kinematic and dynamic methods have not been successful. This is likely due to the fact that additional assumptions were necessary and significant errors were introduced into the control algorithms so that the state variables could be effectively compensated for time delay by using the phase shift method, as was verified experimentally.

Good agreement was obtained between analytical and experimental results. Small discrepancies, however, were present which were primarily due to controller-structure interaction. In the uncontrolled test, the structure motion induced slight actuator displacement which was continuously corrected to zero by the servo-controlled system. Therefore, damping force was a complicated function of the actuator mechanism. However, for the controlled cases, most of the damping force was contributed by the feedback force so that the influence of the interactions was negligible.

Since the controller dynamics was an integral part of the structural dynamics, the structure was no longer a conventional one. As a consequence, the damping factors for the second and third modes were relatively small because of the controller location. The reduced stability margins made the structure vulnerable to instability when these modes remained uncontrolled.

In modal control, the structural stability was very sensitive to modeling errors as modes leaked out to the feedback signals without time delay compensation. Since no perfect filter exists, such leakage could not be eliminated. The leakage, however, could be minimized by passing the control signals through an analog filter at the expense of a larger time delay. Because of control spillover, it is suggested that critical modes be selected in such a way that the residual modes are not excited by the environmental loads.

Since instantaneous optimal control algorithms do not require solving the Riccati matrix equation as required in the classical optimal control, computational advantages exist in the use of instantaneous optimal control. This is particularly evident when the number of degrees of freedom of the structure under control is large.

SECTION 7

REFERENCES

1. Balas, M.J., 'Active Control of Flexible Systems', <u>J. Optimization Theory and Application,</u> <u>25,</u> 1978, pp. 415-436.

2. Chung, L.L., Reinhorn, A.M. and Soong, T.T., 'Experiments on Active Control of Seismic Structures', <u>J. Engineering Mechanics ASCE,</u> <u>114,</u> 1988, pp. 241-256.

3. Chung, L.L., <u>Analysis and Experiments for Practical Application of Active Structural Control,</u> Ph.D. Dissertation, State University of New York at Buffalo, Buffalo, July, 1987.

4. Dehghanyar, T.J., Masri, S.F., Miller, R.K., Bekey, G.A. and Caughey, T.K., 'An Analytical and Experimental Study into the Stability and Control of Nonlinear Flexible Structures', <u>Proc. Fourth VPI and SU/ AIAA Symposium on Dynamics and Control of Large Structures,</u> Blacksburg, Virginia, 1983.

5. Goh, C.J. and Caughey, T.K., 'On the Stability Problem Caused by Finite Actuator Dynamics in the Collocated Control of Large Space Structures', <u>Int. J. Control,</u> <u>41,</u> 1985, pp. 787-802.

6. Leipholz, H.H.E., ed., <u>Structural Control,</u> Martinus Nijhoff, Amsterdam, 1987.

7. Lin, R.C., <u>Experimental Evaluation of Instantaneous Optimal Algorithms for Structural Control,</u> Ph.D. Dissertation, State University of New York at Buffalo, Buffalo, July, 1987.

8. Lin, R.C., Soong, T.T., and Reinhorn, A.M., 'Active Stochastic Control of Seismic Structures', <u>Stochastic Approaches in Earthquake Engineering,</u> (Lin, Y.K. and Minai, R., eds.) Springer-Verlag, New York, 1987, pp. 157-173.

9. Masri, S.F., Bekey, A.A., and Caughey, T.K., 'On-line Control of Nonlinear Flexible Structures', <u>J. Applied Mechanics, ASME,</u> <u>49,</u> 1982, pp. 877-884.

10. McGreevy, S., Soong, T.T. and Reinhorn, A.M., 'An Experimental Study of Time Delay Compensation in Active Structural Control', <u>Proc. SEM 6th International Modal Analysis Conference,</u> Florida, February, 1988.

11. Roorda, J., 'Experiments in Feedback Control of Structures', <u>Structural Control,</u> H.H.E. Leipholz, ed., North Holland, Amsterdam, 1980, pp. 629-661.

12. Sage, A.P. and White, C.C., <u>Optimal Systems Control,</u> second edition, Prentice Hall, New York, 1977.

13. Soong, T.T. and Chang, J.C.H., 'Active Vibration Control of Large Flexible Structures', <u>Shock and Vibration Bulletin,</u> <u>52,</u> 1982, pp. 47-54.

14. Soong, T.T., Reinhorn, A.M. and Yang, J.N., 'A Standardized Model for Structural Control Experiments and Some Experimental Results', Structural Control, (Leipholz, H.H.E., ed.), Martinus Nijhoff, Amsterdam, 1987, pp. 669-693.

15. Yang, J.N., Akbarpour, A. and Ghaemmaghami, P., 'Optimal Control Algorithms for Earthquake-Excited Building Structures', Structural Control, (Leipholz, H.H.E., ed), Martinus Nijhoff, Amsterdam, 1987, pp. 748-761.

16. Yang, J.N., Akbarpour, A., and Ghaemmaghami, P., 'Instantaneous Optimal Control Laws for Tall Buildings Under Seismic Excitation', National Center for Earthquake Engineering Research Technical Report, NCEER-TR-87-0007, June, 1987.

17. Yang, J.N., Akbarpour, A, and Ghaemmaghami, P., 'New Control Algorithms for Structural Control', Journal of Engineering Mechanics, ASCE, 113, 1987, pp. 1369-1386.

18. Yang, J.N., Lang, F.X. and Wong, D., 'Optimal Control of Nonlinear Flexible Structures', J. Applied Mechanics, ASME, 1988 (to appear).

The National Center for Earthquake Engineering Research (NCEER) publishes technical reports on a variety of subjects related to earthquake engineering written by authors funded through NCEER. These reports are available from both NCEER's Publications Department and the National Technical Information Service (NTIS). Requests for reports should be directed to the Publications Department, National Center for Earthquake Engineering Research, State University of New York at Buffalo, Red Jacket Quadrangle, Buffalo, New York 14261. Reports can also be requested through NTIS, 5285 Port Royal Road, Springfield, Virginia 22161. NTIS accession numbers are shown in parenthesis, if available.

NCEER-87-0001   "First-Year Program in Research, Education and Technology Transfer," 3/5/87, (PB88-134275/AS).

NCEER-87-0002   "Experimental Evaluation of Instantaneous Optimal Algorithms for Structural Control," by R.C. Lin, T.T. Soong and A.M. Reinhorn, 4/20/87, (PB88-134341/AS).

NCEER-87-0003   "Experimentation Using the Earthquake Simulation Facilities at University at Buffalo," by A.M. Reinhorn and R.L. Ketter, to be published.

NCEER-87-0004   "The System Characteristics and Performance of a Shaking Table," by J.S. Hwang, K.C. Chang and G.C. Lee, 6/1/87, (PB88-134259/AS).

NCEER-87-0005   "A Finite Element Formulation for Nonlinear Viscoplastic Material Using a Q Model," by O. Gyebi and G. Dasgupta, 11/2/87, (PB88-213764/AS).

NCEER-87-0006   "Symbolic Manipulation Program (SMP) - Algebraic Codes for Two and Three Dimensional Finite Element Formulations," by X. Lee and G. Dasgupta, 11/9/87, (PB88-219522/AS).

NCEER-87-0007   "Instantaneous Optimal Control Laws for Tall Buildings Under Seismic Excitations," by J.N. Yang, A. Akbarpour and P. Ghaemmaghami, 6/10/87, (PB88-134333/AS).

NCEER-87-0008   "IDARC: Inelastic Damage Analysis of Reinforced Concrete-Frame Shear-Wall Structures," by Y.J. Park, A.M. Reinhorn and S.K. Kunnath, 7/20/87, (PB88-134325/AS).

NCEER-87-0009   "Liquefaction Potential for New York State: A Preliminary Report on Sites in Manhattan and Buffalo," by M. Budhu, V. Vijayakumar, R.F. Giese and L. Baumgras, 8/31/87, (PB88-163704/AS).

NCEER-87-0010   "Vertical and Torsional Vibration of Foundations in Inhomogeneous Media," by A.S. Veletsos and K.W. Dotson, 6/1/87, (PB88-134291/AS).

NCEER-87-0011   "Seismic Probabilistic Risk Assessment and Seismic Margins Studies for Nuclear Power Plants," by Howard H.M. Hwang, 6/15/87, (PB88-134267/AS).

NCEER-87-0012   "Parametric Studies of Frequency Response of Secondary Systems Under Ground-Acceleration Excitations," by Y. Yong and Y.K. Lin, 6/10/87, (PB88-134309/AS).

NCEER-87-0013   "Frequency Response of Secondary Systems Under Seismic Excitation," by J.A. HoLung, J. Cai and Y.K. Lin, 7/31/87, (PB88-134317/AS).

NCEER-87-0014   "Modelling Earthquake Ground Motions in Seismically Active Regions Using Parametric Time Series Methods," G.W. Ellis and A.S. Cakmak, 8/25/87, (PB88-134283/AS).

NCEER-87-0015   "Detection and Assessment of Seismic Structural Damage," by E. DiPasquale and A.S. Cakmak, 8/25/87, (PB88-163712/AS).

NCEER-87-0016   "Pipeline Experiment at Parkfield, California," by J. Isenberg and E. Richardson, 9/15/87, (PB88-163720/AS).

NCEER-87-0017   "Digital Simulation of Seismic Ground Motion," by M. Shinozuka, G. Deodatis and T. Harada, 8/31/87, (PB88-155197/AS).

A-1

NCEER-87-0018   "Practical Considerations for Structural Control: System Uncertainty, System Time Delay and Trunca-
tion of Small Control Forces," J. Yang and A. Akbarpour, 8/10/87, (PB88-163738/AS).

NCEER-87-0019   "Modal Analysis of Nonclassically Damped Structural Systems Using Canonical Transformation," by
J.N. Yang, S. Sarkani and F.X. Long, 9/27/87, (PB88-187851/AS).

NCEER-87-0020   "A Nonstationary Solution in Random Vibration Theory," by J.R. Red-Horse and P.D. Spanos, 11/3/87,
(PB88-163746/AS).

NCEER-87-0021   "Horizontal Impedances for Radially Inhomogeneous Viscoelastic Soil Layers," by A.S. Veletsos and
K.W. Dotson, 10/15/87, (PB88-150859/AS).

NCEER-87-0022   "Seismic Damage Assessment of Reinforced Concrete Members," by Y.S. Chung, C. Meyer and M.
Shinozuka, 10/9/87, (PB88-150867/AS).

NCEER-87-0023   "Active Structural Control in Civil Engineering," by T.T. Soong, 11/11/87, (PB88-187778/AS).

NCEER-87-0024   "Vertical and Torsional Impedances for Radially Inhomogeneous Viscoelastic Soil Layers," by K.W.
Dotson and A.S. Veletsos, 12/87, (PB88-187786/AS).

NCEER-87-0025   "Proceedings from the Symposium on Seismic Hazards, Ground Motions, Soil-Liquefaction and
Engineering Practice in Eastern North America, October 20-22, 1987, edited by K.H. Jacob, 12/87,
(PB88-188115/AS).

NCEER-87-0026   "Report on the Whittier-Narrows, California, Earthquake of October 1, 1987," by J. Pantelic and A.
Reinhorn, 11/87, (PB88-187752/AS).

NCEER-87-0027   "Design of a Modular Program for Transient Nonlinear Analysis of Large 3-D Building Structures," by
S. Srivastav and J.F. Abel, 12/30/87, (PB88-187950/AS).

NCEER-87-0028   "Second-Year Program in Research, Education and Technology Transfer," 3/8/88, (PB88-219480/AS).

NCEER-88-0001   "Workshop on Seismic Computer Analysis and Design of Buildings With Interactive Graphics," by J.F.
Abel and C.H. Conley, 1/18/88, (PB88-187760/AS).

NCEER-88-0002   "Optimal Control of Nonlinear Flexible Structures," J.N. Yang, F.X. Long and D. Wong, 1/22/88,
(PB88-213772/AS).

NCEER-88-0003   "Substructuring Techniques in the Time Domain for Primary-Secondary Structural Systems," by G. D.
Manolis and G. Juhn, 2/10/88, (PB88-213780/AS).

NCEER-88-0004   "Iterative Seismic Analysis of Primary-Secondary Systems," by A. Singhal, L.D. Lutes and P. Spanos,
2/23/88, (PB88-213798/AS).

NCEER-88-0005   "Stochastic Finite Element Expansion for Random Media," P. D. Spanos and R. Ghanem, 3/14/88,
(PB88-213806/AS).

NCEER-88-0006   "Combining Structural Optimization and Structural Control," F. Y. Cheng and C. P. Pantelides, 1/10/88,
(PB88-213814/AS).

NCEER-88-0007   "Seismic Performance Assessment of Code-Designed Structures," H.H-M. Hwang, J-W. Jaw and H-J.
Shau, 3/20/88, (PB88-219423/AS).

NCEER-88-0008   "Reliability Analysis of Code-Designed Structures Under Natural Hazards," H.H-M. Hwang, H. Ushiba
and M. Shinozuka, 2/29/88.

NCEER-88-0009   "Seismic Fragility Analysis of Shear Wall Structures," J-W Jaw and H.H-M. Hwang, 4/30/88.

NCEER-88-0010   "Base Isolation of a Multi-Story Building Under a Harmonic Ground Motion - A Comparison of Performances of Various Systems," F-G Fan, G. Ahmadi and I.G. Tadjbakhsh, 5/18/88.

NCEER-88-0011   "Seismic Floor Response Spectra for a Combined System by Green's Functions," F.M. Lavelle, L.A. Bergman and P.D. Spanos, 5/1/88.

NCEER-88-0012   "A New Solution Technique for Randomly Excited Hysteretic Structures," G.Q. Cai and Y.K. Lin, 5/16/88.

NCEER-88-0013   "A Study of Radiation Damping and Soil-Structure Interaction Effects in the Centrifuge," K. Weissman, supervised by J.H. Prevost, 5/24/88, to be published.

NCEER-88-0014   "Parameter Identification and Implementation of a Kinematic Plasticity Model for Frictional Soils," J.H. Prevost and D.V. Griffiths, to be published.

NCEER-88-0015   "Two- and Three-Dimensional Dynamic Finite Element Analyses of the Long Valley Dam," D.V. Griffiths and J.H. Prevost, 6/17/88, to be published.

NCEER-88-0016   "Damage Assessment of Reinforced Concrete Structures in Eastern United States," A.M. Reinhorn, M.J. Seidel, S.K. Kunnath and Y.J. Park, 6/15/88.

NCEER-88-0017   "Dynamic Compliance of Vertically Loaded Strip Foundations in Multilayered Viscoelastic Soils," S. Ahmad and A.S.M. Israil, 6/17/88.

NCEER-88-0018   "An Experimental Study of Seismic Structural Response With Added Viscoelastic Dampers," R.C. Lin, Z. Liang, T.T. Soong and R.H. Zhang, 6/30/88.

NCEER-88-0019   "Experimental Investigation of Primary - Secondary System Interaction," G.D. Manolis, G. Juhn and A.M. Reinhorn, 5/27/88, to be published.

NCEER-88-0020   "A Response Spectrum Approach For Analysis of Nonclassically Damped Structures," J.N. Yang, S. Sarkani and F.X. Long, 4/22/88.

NCEER-88-0021   "Seismic Interaction of Structures and Soils: Stochastic Approach," A.S. Veletsos and A.M. Prasad, 7/21/88, to be published.

NCEER-88-0022   "Identification of the Serviceability Limit State and Detection of Seismic Structural Damage," E. DiPasquale and A.S. Cakmak, 6/15/88.

NCEER-88-0023   "Multi-Hazard Risk Analysis: Case of a Simple Offshore Structure," B.K. Bhartia and E.H. Vanmarcke, 7/21/88, to be published.

NCEER-88-0024   "Automated Seismic Design of Reinforced Concrete Buildings," Y.S. Chung, C. Meyer and M. Shinozuka, 7/4/88, to be published.

NCEER-88-0025   "Experimental Study of Active Control of MDOF Structures Under Seismic Excitations," L.L. Chung, R.C. Lin, T.T. Soong and A.M. Reinhorn, 7/10/88.